Supplementary materials

Methods

Animals: Animals were obtained from Jackson Laboratories (Bar Harbor, Maine, USA), Charles River (France), or Taconic (Denmark), were maintained in a temperature- and humidity-controlled environment, and were subject to a 12-h light/dark cycle. Unless otherwise stated, the animals had *ad libitum* access to food and water. With the exception of untreated animals used for primary cell isolation, all animals were injected s.c. or i.v. with vehicle, semaglutide, or liraglutide. Prior to the start of treatment in all studies, animals were distributed into groups according to BW to minimize statistical variations between groups.

For IHC and electron microscopy experiments, adult Sprague-Dawley rats weighing 250−280 g were used. Animals were housed under standard conditions (lights on between 06.00 and 18.00 h, temperature 22±1 °C, mouse chow and water *ad libitum*). All experimental protocols were reviewed and approved by the Animal Welfare Committees at the Institute of Experimental Medicine of the Hungarian Academy of Sciences.

Rats were anaesthetized with a mixture of ketamine and xylazine (ketamine 50 mg/kg, xylazine 10 mg/kg body weight, intraperitoneally) and were perfused transcardially with 30 ml 0.01 M phosphate-buffered saline pH 7.4 (PBS), followed by 150 ml 3% paraformaldehyde (PFA) and 1% acrolein in 0.1 M phosphate buffer (PB) pH 7.4. The brains were rapidly removed.

Weight loss, food preference, and calorimetry studies in obese rodents: Animals were single-housed and mock-handled prior to the start of treatment. DIO mice (male C57BL/6J) were fed a high-fat diet containing either 45% or 60% kcal from fat (Research Diets D12451, New Brunswick, NJ) from 4 w of age and were treated with compound after approximately 20 w. DIO female Wistar rats were put on a diet of *ad libitum* chow (Altromin 1324, Brogaarden, Denmark) and chocolate at arrival. BW and food intake were measured manually on a daily basis during the treatment period.

In the study described in Figures 1A and B, male C57BL/6J diet-induced obese (DIO) mice were maintained on a 45% kcal fat diet (Research Diets D12451, New Brunswick, NJ) and doses for the 10, 30, and 100 nmol/kg groups were escalated over a 2−4-d period at a rate of 3, 10, 30, and 100 nmol/kg, as appropriate.

In the DIO rat food-preference study (Figure 1C−E), female Wistar rats were offered *ad libitum* chow (Altromin 1324, Brogaarden, Denmark) and chocolate. Every day one of five different variants of commercially available Marabou milk chocolate bars (Plain, Daim, Roasted Nuts, Non-stop and Digestive) was offered ad libitum along with ad libitum chow. The composition of the different chocolate bars varied slightly, with energy content around 2300 KJ/100 g, sugars 50−60 g/100 g and fat 30−40 g/100 g. Chow was placed in the lid of the cage and chocolate was placed inside the cage. In order to encourage a large energy intake in the rats, the five different kinds of chocolate bars were offered with daily alternation. The rats preferred eating the chocolate, resulting in more than 90% of calories being consumed as chocolate. Treatment was initiated after 9 mo on the chow/chocolate diet.

In the indirect calorimetry study (Figure 1F−K), single-housed male DIO C57BL/6J mice on the 45% kcal fat diet described above were acclimated to the sealed cage environment of the calorimetry chambers (TSE Systems Phenomaster, Germany) for 11 d, prior to the start of treatment. Energy intake, energy expenditure (EE), respiratory exchange ratio, and locomotor activity were measured by the system every 10 min during the mock-handling and treatment periods. EE was calculated in kcal/h by the TSE calorimetry system according to the Weir equation. Average dark-phase and light-phase values and daily food intake for each individual animal and groups were calculated. Note that the semaglutide dose was escalated over a 4-d period at a rate of 1, 3, 10, and 40 μg/kg. For the weight-matched group, food was adjusted on a daily basis depending on the weight loss observed in the semaglutide treatment group and based on similar historic studies.

For the mouse quantitative PCR (qPCR) study, 20-week-old male DIO mice (C57bl/6J, the Jackson Laboratories, on a 60% kcal fat diet from Research Diets D12492, New Brunswick, NJ) were divided into three weight-matched groups (n=12). All animals were s.c. dosed for 18 d with either vehicle (*ad libitum* fed and weight matched) or semaglutide (0.15 mg/kg). Semaglutide treatment was up-titrated with 33%, 66%, and 100% for the first three doses. The weight-matched group was food restricted to be weight matched to the semaglutide-treated group.

In the DIO rat transcriptomic study, 24-week-old male DIO rats were used. The animals were treated with vehicle, liraglutide (~0.6 mg/kg), semaglutide (~0.06 mg/kg), or were weight-matched animals, as described above, for 23 d (n=16/group). Doses of liraglutide

and semaglutide were adjusted to give a weight loss of ~12%. The rats were fed a 60% kcal fat diet until 22 weeks of age, and a 45% kcal fat diet thereafter.

Distribution of semaglutide^{Cy3} and co-lozalization studies: Fluorescently labeled semaglutide and liraglutide were synthesized by conjugating Cyanine 3 (Cy3) (Lumiprobe) to the peptides. Semaglutide^{Cy3}, liraglutide^{Cy3}, or vehicle (PBS) were injected i.v. (tail) into male C57BL/6J mice (n=3/3/2) daily for 4 d (30 nmol/kg d 1, 60 nmol/kg d 2+3, 120 nmol/kg d 4); 6 h after the last dose, the mice were anesthetized using isoflurane, and euthanized using cardiac perfusion with first saline followed by 4% PFA. The mice brains were collected and post fixated in 4% PFA at RT overnight. After post fixation, the brains were saturated in 25% sucrose solution, frozen and cryosectioned coronally at 35 µm into six series. One series from each mouse was stained with DAPI (1:1000) for detection of peptide localization. The remaining series were used for free floating IHC. Confocal images from hypothalamic arcuate nucleus (ARH), paraventricular nucleus of the hypothalamus (PVH), dorsomedial hypothalamic nucleus (DMH), and area prostrema (AP)/nucleus tractus solitarius (NTS) were acquired with the Leica Confocal Imaging System TCS SP8. Liraglutide^{Cy3} and semaglutide^{Cy3} distribution and co-expression were visualized using confocal imaging. Images from the ARH and AP/NTS were acquired using the Leica Confocal Imaging System TCS SP8 with the HC PL APO 20x/0.75 objective. Confocal Z-stacks were acquired ranging between 12–25 µm with laser excitation in sequential mode, corresponding to either DAPI, 488, Cy3, or Cy5 from the region of interests. The Z-stacks were then processed into maximum projection images using the Leica Application Suite (LAS X) software.

Whole-brain compound distribution: Fluorescently labeled semaglutide (semaglutide^{VT750}) was synthesized in house by conjugating VivoTag-S®750 NIR FLUOROCHROME LABEL (Perkin Elmer) to the peptide. Male mice (C57BL/6J [n=4] or *Glp-1r-/-* [n=5]) received a single i.v. dose of semaglutide^{VT750} 30 nmol/kg or were sub-chronically dosed s.c. (C57BL/6J [n=4]) once-daily (10 nmol/kg d 1, 20 nmol/kg d 2, 30 nmol/kg d 3−5); 6 h after the single or last injection, the mice were euthanized using cardiac perfusion with heparinized (10 U/ml) saline for 2 min, followed by neutral buffered formalin (NBF, 10%) for 10 min, with a flow rate of 5 ml/min. The brains were fixed in NBF at RT overnight and subsequently cleared using a modified 3DISCO protocol (1). Male mice C57BL/6J (n=4) were sub-chronically dosed with liraglutide^{VT750} once-daily (10 nmol/kg d 1, 20 nmol/kg d 2, 30 nmol/kg d 3−5); had brains collected and processed in the same manner as those receiving semaglutide^{VT750}.

Whole-brain c-Fos and glucagon-like peptide-1 receptor (GLP-1R) staining: C57BL/6J male mice (n=6) were s.c. injected with semaglutide (0.01 mg/kg) or vehicle. Mice were euthanized 4 h after injection using isoflurane followed by cardiac perfusion with 4% PFA. Brains were excised and post fixed in 4% PFA overnight at RT and transferred stepwise to 100% methanol using the following protocol: 20% methanol (in double distilled water) for 1 h, 40% methanol for 1 h, 60% methanol for 1 h, 80% methanol for 1 h, and 100% methanol for 1 h, twice. iDISCO staining was performed as previously described (2), with one exception: all the washing steps after incubation with primary and secondary antibody were extended from 1 to 3 d. Incubation time for primary and secondary antibody was 4 d each for c-Fos staining and 7 d each for GLP-1R staining.

Connectivity analysis: Brain connectivity maps (n=2,469), based on enhanced green fluorescent protein (EGFP)-expressing adeno-associated viral vectors to trace axonal projections from defined regions and cell types, were downloaded from AIBS (http://www.brain-map.org/). Similarity was computed between the average semaglutide-specific c-Fos increase and each individual connectivity map, based on percentage of overlap between binary versions of the data sets. The connectivity maps were ranked by increasing overlap with the semaglutide-specific c-Fos increase.

Light sheet imaging: Brain samples were scanned using an UltraMicroscope II LSFM system (Lavision Biotec, Bielefeld, Germany) in 10.32 µm isotropic resolution for the semaglutide^{VT750} distribution study and 4.06 µm for the c-Fos activation study and the GLP-1R staining. For labeled peptides, data acquisition was performed using a 620 nm emission filter to acquire autofluorescence, and a 710 nm emission filter to acquire specific signals. With whole-brain c-Fos staining and GLP-1R staining the autofluorescence was recorded at 545 nm, while the c-Fos signal was acquired with a 620 nm emission filter.

Electrophysiology: Seven POMC-EGFP and four NPY-hrGFP male mice (Jackson Laboratories) aged 6−10 w were used for all recordings. Coronal slices containing ARH were prepared.

Isolation of primary astrocytes, endothelial cells, and tanycytes: All animals used for primary cell isolations were euthanized without prior treatment. Rat primary astrocytes were isolated from 2−4-d-old Sprague Dawley rats (Taconic, Ejby, Denmark) following a previously described protocol (3). Brain capillary endothelial cells were isolated from the cortices of calves less than 12 months of age, obtained from a

slaughterhouse (Mogens Nielsen Kreaturslagteri A/S, Herlufmagle, Denmark), as previously described (4). Rat tanycytes were isolated from 10-d-old Sprague Dawley rats, as previously described (5), with some modifications: 30 rat pups were decapitated and the median eminence (ME) were microdissected and pooled into tanycyte DMEM (TDMEM) consisting of DMEM (41965-039, Gibco) supplemented with 1% (v/v) of penicillin/streptomycin and L-glutamine solutions (both Gibco) and 10% donor bovine serum (16030-074, Gibco). The collected MEs were dispersed through a 20 µm nylon net filter (Millipore), seeded in a T75 flask and cultured for 10 d before initial change to fresh TDMEM. Fresh TDMEM was then applied every 2−3 d for an additional week of culture.

Establishment of blood-brain barrier (BBB) and tanycyte-models: Bovine brain endothelial cells were prepared from cortices of calves aged <12 m (Mogens Nielsen Kreaturslagteri A/S, Herlufmagle, Denmark). Astrocytes were from 2-4-d-old rat pups, while tanycytes were from 10-d-old rat pups (Sprague Dawley, Taconic). Endothelial cells and astrocytes were cultured and applied in contact co-culture to establish BBB models, as previously described (4, 6-8), with the modification that 4 µg/ml puromycin was added to the culture medium the first 2 d of endothelial cell culture. The purity and identity of the cells were routinely verified by the presence of vWF and glial fibrillary acidic protein in the endothelial cells and astrocytes, respectively, as previously demonstrated (4). Tanycytes were passaged and seeded in mono-cultures on coated permeable supports (90,000 cells/cm^2) 17 d after isolation. The tanycytes were cultured for 4 d in TDMEM followed by 3 d in serum-free tanycyte-defined medium consisting of DMEM/F12 with 15 mM HEPES (D6434, Sigma-Aldrich) + penicillin/streptomycin (Gibco) + L-glutamine (Gibco) + bovine insulin (5 µg/ml) (Sigma-Aldrich) + putrescine (100 µM) (Sigma-Aldrich). The identity and purity of the tanycytes were verified by the presence of vimentin and G-protein-coupled receptor 50 (GPR50) and the absence of glial fibrillary acidic protein (Supplementary Figure 2).

In vitro uptake of semaglutide^{Cy3} or ^{125}I-semaglutide and immunofluorescence: On the experimental day (d 6 on permeable supports for the BBB model and d 7 for tanycytes), the culture medium was replaced with a defined-uptake buffer consisting of Hank's balanced salt solution with calcium and magnesium (Gibco) supplemented with 0.1% ovalbumin (Sigma-Aldrich), 0.005% Tween 20, and 10 mM HEPES (Gibco) (pH set to 7.4). The cells were pre-incubated for 15 min at 37°C with shaking in either clean uptake buffer or uptake buffer + 1000 nM exendin 9-39. For uptake of semaglutide^{Cy3}, the cells were added either to clean uptake buffer (control) or uptake buffer + semaglutide^{Cy3} (final concentration 100 nM) to both compartments and incubated for 1 h at 37°C in motion. For uptake of ^{125}I-semaglutide, the cells were added to uptake buffer

containing 0.7 nM ^{125}I-semaglutide (1 µCi/ml) with or without 1000 nM exendin 9-39 in the apical compartment and uptake buffer with or without 1000 nM exendin 9-39 in the basolateral compartment. The cells were incubated for 30 min at 37°C in motion to accumulate ^{125}I-semaglutide. Receiver and donor samples were withdrawn and the uptake buffer was aspired. The cells were washed three times in ice-cold uptake buffer. The supports from the isotope experiments were either cut out directly to measure the amount of uptake or added to fresh, pre-heated uptake buffer to subsequently measure release. The cells for the release studies were incubated for up to 1 h in uptake buffer. The permeable supports were placed into a picocount scintillation plate (PicoPlate-96, Perkin Elmer) and counted in a TopCount NXT scintillation counter (Perkin Elmer). Resulting counts per min were converted to molar quantities by comparison with a standard curve of ^{125}I-semaglutide in uptake buffer run in parallel. The quantities were standardized relative to the individual donor solutions, so that the amount of compound taken up, relative to the amount added could be determined. All quantitative values are based on triplicates and presented with means and SD.

Cells for immunofluorescence were fixed in 4% PFA, permeabilized in 0.1% Triton x-100 and blocked in PBS + 2% BSA. Samples from uptake experiments with semaglutide^{Cy3} were subsequently incubated with Hoechst (1 µg/ml). Samples for IHC were incubated with antibody overnight at 4°C, washed, and incubated with secondary antibodies combined with Hoechst (1 µg/ml) for 1 h at RT. The cells were mounted on coverslips and visualized using a Leica SP8 confocal microscope (Leica DMi8).

Tissue preparation for ultrastructural studies

Serial 25 µm thick coronal sections were cut through the whole brain on a Leica VT 1000S vibratome (Leica Microsystems, Wetzlar, Germany). The sections were collected in 0.1 M PBS (pH 7.4), transferred into anti-freeze solution (30% ethylene glycol; 25% glycerol; 0.05 M PB) and stored at −20°C. The sections were then washed with PBS, treated with 1% sodium borohydride in 0.1M PB for 30 min and with 0.5% H2O2 in PBS for 15 min, cryoprotected in 15% sucrose in PBS for 30 min at RT and in 30% sucrose in PBS overnight at 4°C, quickly frozen over liquid nitrogen and thawed three times to improve antibody penetration into the tissue. The pre-treated sections were incubated in 2% NHS (diluted in 0.1M PBS) for 20 min and then placed in mouse monoclonal anti-GLP-1R antibody (0.5 µg/ml) in 2% NHS for 4 d at 4 °C. After rinsing in PBS, the sections were incubated in biotinylated donkey anti-mouse IgG (Jackson Laboratories) diluted at 1:500 in 2% NHS overnight at 4°C. After washing in PBS, the sections were then treated with avidin-biotin-peroxidase complex (ABC Elite, 1:1000, Vector Laboratories) and the GLP-1R immunoreactivity was developed in Ni-DAB developer

(0.05% diaminobenzidine and 0.15% nickel-ammonium sulphate/0.005% H_2O_2 in 0.05 M Tris buffer, pH 7.6). The sections were rinsed in 0.2 M sodium citrate pH 7.5, and the nickel particles were intensified with the Gallyas silver intensification method for 3 mins. Finally, the sections were placed in 0.05% gold-chloride for 10 mins, washed in 0.2 M sodium citrate, pH 7.5, and in 3% sodium-thiosulphate solution for 10 mins, with each step completed at RT.

Embedding and ultrastructural examination of the immunostained sections
Sections were osmicated for 60 mins at RT, and then treated with 2% uranyl acetate in 70% ethanol for 30 min. Following dehydration in an ascending series of ethanol and acetonitrile (Sigma), the sections were flat embedded in Durcupan ACM epoxy resin (Fluka) on liquid release agent (Electron Microscopy Sciences)-coated slides and polymerized at 56 °C for 2 d. After polymerization, 60–70 nm thick ultrathin sections were cut with a Leica UCT ultramicrotome (Leica Microsystems, Wetzlar, Germany). The ultrathin sections were mounted onto Formvar-coated, single-slot grids, treated with lead citrate and examined with a JEOL-100 C transmission electron microscope. Specificity of the antibody was determined with the rabbitized version of the antibody. No signal was detected.

Gene expression analysis: Animals for gene expression analysis were euthanized in the morning the day after the last dose. Animals were anesthetized with isoflurane and decapitated. The brains were rapidly dissected, frozen on powdered dry ice, and stored at −80°C until further processing. Coronal sections (10 µm) were cut on a cryostat using systematic uniform random sampling techniques. Sections were mounted on cold polyethylene naphthalate (PEN) Membrane Glass Slides (Leica Microsystems). For mouse brains, a series of sections covering the ARH were collected approximately from bregma −1.31 mm to −2.53 mm (9). For rat brains, four series of sections were collected: (1) lateral sulcus (LS) approximately from bregma 1.28 mm to −0.24 mm (10); (2) PVH approximately bregma −1.32 mm to −1.92 mm; (3) ARH (including the DMH) approximately bregma −1.92 mm to −3.84 mm; and (4) AP (including the NTS) approximately bregma −13.68 mm to −14.28 mm. Following sectioning, slides were stored at −80°C until further processing. During laser capture microdissection (LCM), tissue representing one stereological sampling of each area was processed at a time. Prior to LCM, sections were thawed for approximately 3 min at 4°C. The sections were then stained for 5 min at 4°C in a 0.1% cresyl violet acetate solution (Sigma-Aldrich) dissolved in 70% ethanol. Sections were subsequently dehydrated in a graded ethanol series and air-dried for approximately 3 min in a fume hood. Using a Leica LMD7 (Leica Microsystems), the relevant area was identified and collected. For mouse tissue, the

PicoPure™RNA Isolation Kit (Arcturus, Applied Biosystems™) was used for cell lysis and RNA purification. For rat tissue, the RNeasy Plus Kit (Qiagen) was used for cell lysis and RNA purification. Following LCM, the remaining tissue from at least one series per animal was scraped off and used for assessment of RNA quality using an Agilent Bioanalyzer. The mouse and rat tissue had average RNA Integrity Number (RIN) values of 7.2 ± 0.5 and 8.7 ± 0.7, respectively. The remaining tissue from at least one series per animal was scraped off and used for assessment of RNA quality using an Agilent Bioanalyzer. RNASeq libraries were prepared using a SMART-Seq v4 Ultra Low Input RNA Kit and Low Input Library Prep Kit v2 (Illumina; San Diego, USA), and sequenced using the Illumina HiSeq 2500. Twelve samples were sequenced per lane (100 bp paired end reads).

qPCR analysis: cDNA synthesis was performed using 4 µl target RNA and 1 µl Superscript VILO Master Mix (Thermo Fisher Scientific), as recommended. The qPCR reactions were run in duplicate on a Viia7 instrument (Thermo Fisher Scientific), and prepared by mixing 7.5 µl TaqMan Gene Expression MasterMix (Thermo Fisher Scientific), 0.5 µl Taqman assay, and 2 µl cDNA (pre-diluted 15 times). Protocol: 95°C for 10 min, 40 cycles of 95°C for 15 s, and 60°C for 1 min. Probes used for Taqman assays: agouti-related peptide (AgRP), Mn00475829; cocaine- and amphetamine-regulated transcript (CART), Mm00489086; pro-opiomelanocortin (POMC), Mm00435874; neuropeptide-Y (NPY), Mm00445771; β2-microglobulin (B2m), Mm00437762; Tyrosine 3-Monooxygenase/Tryptophan 5-Monooxygenase Activation Protein, Zeta (Ywhaz), Mm01158417; Ubiquitin C (Ubc), Mm01198158; Ribosomal Protein Large P0 (Rplp0), Mm99999223; Ribosomal Protein S18 (Rps18), Mm02601777; Phosphoglycerate Kinase 1 (Pgk1), Mm01225301. The average cycle of quantification (Cq) of the two technical replicates for each sample and gene was used for further calculation. The relative expression values were calculated across samples according to the formula $2^{-(Cq-Cqmin)}$ (using the $2^{-\Delta\Delta Ct}$ method (11)), where Cqmin was the lowest measured Cq value for the gene across samples. For each sample, a numeric scaling factor was determined by calculating the geometric mean of the relative expression values of the six housekeeping genes in the samples. Subsequently, the relative expression values for each gene and sample were divided by this sample-specific scaling factor to normalize for differences in RNA content in the experiment.

For the RNA sequencing (RNAseq) analysis, libraries were prepared using Illumina's SMART-Seq v4 Ultra Low Input RNA Kit and Low Input Library Prep Kit v2 (Illumina; San Diego, USA) and sequenced using the Illumina HiSeq 2500 platform. Twelve samples were sequenced per lane (100 base pair [bp] paired-end reads). RNAseq was conducted by Eurofins Genomics, Ebersberg, Germany. Overall read quality was assessed using

FastQC v0.10.0 (http://www.bioinformatics.babraham.ac.uk/projects/fastqc/) and, based on this, the following pre-processing/cleanup steps were performed using the Fastx toolkit v0.0.13 (http://hannonlab.cshl.edu/fastx_toolkit/license.html) and PRINSEQ (12): (1) 5 nt were clipped off from the 5' end of every read; 2) the 3´ end was trimmed to Q30; (3) the reads were filtered to remove all reads with 'N's; and (4) the reads were filtered to an average of Q25 or above and 70 bp length. Reads were then mapped with the STAR aligner v2.5.2a (13) to the rat genome rn6 ensembl release 86, where the duplicate NPY gene (ENSRNOG00000046449) had been masked from the genome sequence and removed from the gene annotation file. Read counts were imported into R, and DESeq2 (14) was used to identify differential expression and to transform read counts into variance stabilized expression values for quality control (QC) and visualizations. During QC, samples with less than 5 mio reads total or where <45% mapped to the rat genome where discarded. Furthermore, principal components analysis (PCA) and correlation analyses were used to identify and exclude additional outlier samples. Specifically, for PCA, samples that did not group together with samples from the same tissue were excluded according to the first principal component deviating more than 1xSD, or the second principal component deviating more than 3xSD from the sample's four closest neighbors. Moreover, samples within tissue group Pearson correlations <0.75 were excluded.

IHC: Primary antibodies used included: two anti-GLP-1R monoclonal antibody (7F38A2, Novo Nordisk), one mouse monoclonal and the other rabbit monoclonal (where the variable regions of the heavy and light chain from the mouse monoclonal GLP-1R antibody were grafted onto a rabbit IgG); SST (Rat anti Human SST, 8330-0009, Biorad); TH (rb anti TH, P40101-150, Pel Freez Biologicals); CART (rb anti CART (55-102), H-003-62, Phoenix Pharmaceuticals); melanin-concentrating hormone (MCH; rb anti MCH, H-070-47, Phoenix Pharmaceuticals); Orexin (rb anti orexin, H-003-30, Phoenix Pharmaceuticals); PrRP (rbPrRP-31, H-008-52, Phoenix Pharmaceuticals); Phospho-CREB (rb anti p-CREB (Ser133) (87G3) 9198, Cell Signaling Technology); vimentin (chicken anti vimentin, AB5733, Millipore); GPR50 (rb anti GPR50 (SE7604, Servier); ZO-1 (ms anti ZO-1, 33-9100, Invitrogen); GFAP (rb anti GFAP, 20334, Dako); c-Fos (rb pAb anti c-Fos (Ab-5) (4-17), Calbiochem). Secondary antibodies used were: Goat anti-Rabbit IgG (H+L) Cross-Adsorbed Secondary Antibody, Alexa Fluor 488 and 546 (A-11008 and A-11010, Invitrogen); Goat anti-mouse IgG (H+L) Cross-Adsorbed Secondary Antibody, Alexa Fluor 488 and 546 (A-11001 and A-11003 Invitrogen); Goat anti-chicken IgY (H+L) Secondary Antibody, Alexa Fluor 488 (A-11039, Invitrogen). Cy5-anti rabbit (Jackson Immunoresearch).

Tyrosine hydroxylase (TH)/somatostatin (SST) single IHC, free floating: (1) PBS, 3x3 min; (2) NBF, 20 min; (3) PBS, 3x10 min; (4) Dualblock, 5 min; (5) PBS, 3x5 min; (6) avidin, 10 min; (7) PBS, 3x5 min; (8) biotin, 10 min; (9) PBS, 3x5 min; (10) blocking buffer (PBS with 4% goat serum, 4% donkey serum, and 3% Triton X-100 [Tx]), 20 min; (11) rbTH antibody (Ab) 1:1000 or rbSST Ab 1:500 in blocking buffer overnight; (12) PBS, 3x10 min; (13) Cy2 do anti-rb 1:200 + Hoechst 1:1000 in blocking buffer, 2 h; (14) PBS, 3x5 min; mount with mounting media.

CART single IHC, free floating: as above, but without avidin/biotin block. Primary Ab: rbCART 1:1000; secondary Ab: Cy5 do anti-rb 1:200.

GLP-1R single IHC, free floating: as above from 1 to 10, then: (11) msGLP-1R Ab 1:500 in blocking buffer overnight; (12) Vectastain ABCcomplex in 0.5% blocking buffer (0.1 M Tris-HCl, pH 7.5, 0.15 M NaCl, 0.5% [w/v] blocking reagent, PerkinElmer FP1020; TNB), 30 min; (13) PBS, 3x10 min; (14) Cy5 do anti-rb 1:50 in amplification buffer, 6 min; (15) PBS, 3x10 min; (16) DAPI 1:1000 in water, 2 min; and (17) PBS, 3x5 min; mount with mounting medium.

Prolactin-releasing peptide (PrRP) single IHC, free floating: (1) PBS with 0.3% Tx, 3x3 min; (2) 0.5% TNB, 1 h; (3) rb-PrRP-31 1:500 in 0.5% TNB overnight at 4°C; (4) HydrogenPeroxid 1% in PBS, 30 min; (5) PBS with 0.3%Tx, 2x3 min; (6) Bright Vision (HRP rb lab. polymer + Hoechst 1:1000), 30 min; (7) PBS with 0.3% Tx, 3x3 min; (8) Cy3-TSA sub. 1:100 in amplification diluent, 15 min; and (9) PBS with 0.3%Tx, 3x3 min; mount with mounting media.

PrRP + GLP-1R double IHC, free floating: (1) PBS, 3x3 min; (2) NBF, 20 min; (3) PBS, 3x10 min; (4) Dualblock, 5 min; (5) PBS, 3x5 min; (6) avidin, 10 min; (7) PBS, 3x5 min; (8) biotin, 10 min; (9) PBS, 3x5 min; (10) blocking buffer (PBS with 4% goat serum, 4% donkey serum, and 3% Tx), 20 min; (11) anti-GLP1-R mouse Ab biotinylated 1:500 in blocking buffer overnight; (12) PBS, 3x10 min; (13) Secondary Cy2 anti-ms 1:200, 1 h; (14) Vectastain ABCcomplex in 0.5% TNB, 30 min; (15) PBS, with 0.3% Tx, 3x3 min; (16) 0.5% TNB, 1 h; (17) rb-PrRP-31 1:500 in 0.5% TNB overnight; (18) HydrogenPeroxid 1% in PBS, 15 min; (19) Bright Vision (HRP rabbit lab. polymer + Hoechst 1:1000), 30 min; (20) PBS with 0.3%Tx, 3x3 min; 21) Cy3-TSA sub. 1:100 in amplification diluent, 15 min; and (22) PBS with 0.3%Tx, 3x3 min; mount with mounting media.

CART + GLP-1R double IHC, free floating: as above from 1 to 12, then: (13) Vectastain ABC complex in 0.5% TNB, 30 min; (14) PBS, 3x10 min; (15) Tyramide Signal Amplification (TSA/488) 1:50 in amplification buffer, 6 min; (16) PBS, 3x10 min; (17) rbCART 1:1000 in blocking buffer overnight; (18) PBS 3x10 min; (19) Donkey anti-rb Cy5 + Hoechts 1:1000 in blocking buffer, 2 h; and (20) PBS, 3x5 min; mount with mounting media.

Chemicals for IHC: PBS (14200-067, Gibco); Tx (Sigma-aldrich); Hoechst (33258, Invitrogen/ThermoFisher), Mounting medium (S3023, Dako); Bright Vision system -HRP rb (VWRKDPVR110HRP, ImmunoLocic VWR); Cy3-TSA substrate (SAT704B001EA, Perkin Elmer); Vectastain ABC kit (PK-6100, Vector); Dualblock (S2003, Dako); Avidin/biotin (004303, Life Technologies); Donkey and goat serum (017-000-121 and 005-000-121, Jackson Immuno Research).

Statistics: Statistical analyses were performed using GraphPad Prism version 7.00 (GraphPad Software Inc, La Jolla, CA, USA). For image analysis: region-of-interest-based comparisons of total fluorescence signal (Figure 2), and c-Fos heat map intensities (Figure 6) were computed using multiple t tests, assuming unequal variance. The c-Fos heat maps were generated as previously described (15). Statistical significance was determined by correcting for multiple comparisons using an FDR of 5% for labeled peptides (Figure 2) and 20% for heat maps based on whole mount-stained samples (Figure 6). A P value less than 0.05 was considered significant using one-way ANOVA.(15)

Supplementary figures and tables

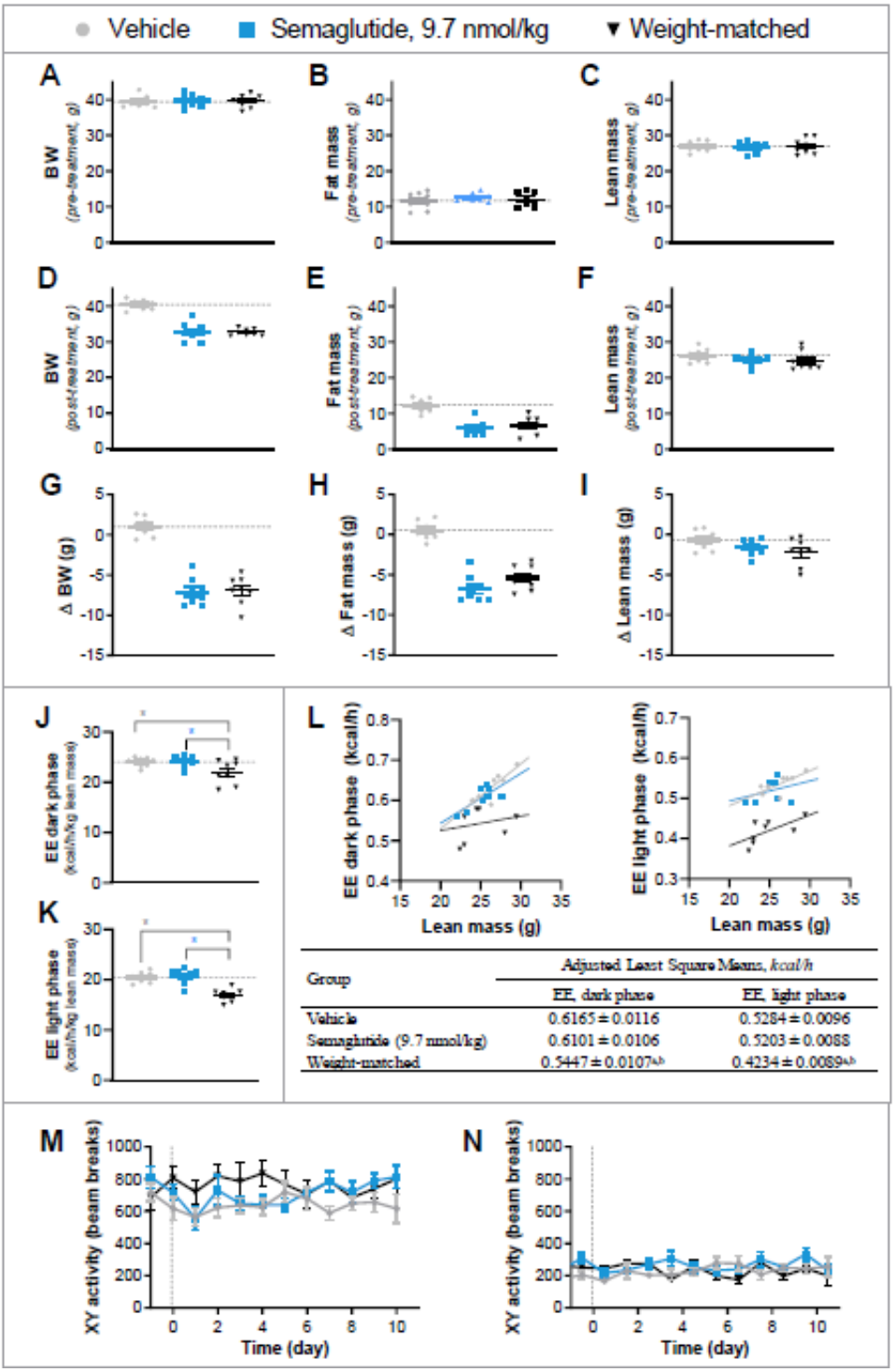

Group	Adjusted Least Square Means, *kcal/h*	
	EE, dark phase	EE, light phase
Vehicle	0.6165 ± 0.0116	0.5284 ± 0.0096
Semaglutide (9.7 nmol/kg)	0.6101 ± 0.0106	0.5203 ± 0.0088
Weight-matched	0.5447 ± 0.0107[a,b]	0.4234 ± 0.0089[a,b]

Supplementary Figure 1. Body composition, EE and locomotor activity. Body weight, lean mass and fat mass as assessed by MR scans of animals pre- **(A-C)**, post-treatment **(D-F)** and change (post minus pre, **G-I**). EE post-treatment normalized to lean mass post-treatment, during light (**J**) and dark **(K)** phases. **(L)** Linear regression plots between EE and lean mass at post-treatment, and adjusted least square means for EE from ANCOVA adjusted for lean mass. Data in the table are mean ± SEM; [a]Significant difference from vehicle; [b]Significant difference from semaglutide. Locomotor (XY) activity

during the calorimetry study in DIO mice during dark **(M)** and light **(N)** phases. No significant differences were detected among groups. BW, body weight; EE, energy expenditure; MR, magnetic resonance; SEM, standard error of the mean.

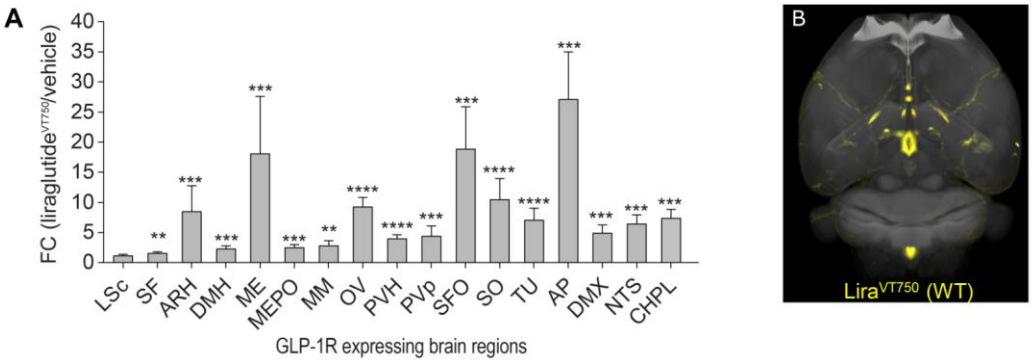

Supplementary Figure 2. Steady-state distribution of liraglutide^{VT750} in mouse brain. (**A**) Bar graph showing mean fold change (FC) and SD of total fluorescence signal in selected brain regions comparing liraglutide^{VT750} (n=4) and vehicle (n=4), after 5 d of daily dosing with fluorescent peptide. Choroid plexus (CHPL) included as a non-GLP-1R-expressing region. $^{**}P \leq 0.01$; $^{***}P \leq 0.001$; $^{****}P \leq 0.0001$. (**B**) Liraglutide^{VT750} (lira ^{VT750}) distribution in mouse brain. Maximum intensity projection of the average signal computed from individual brains (n=4). Steady-state liraglutide^{VT750} signal, wild-type (WT) mice. AP, area postrema; ARH, arcuate nucleus; DMH, dorsomedial hypothalamic nucleus; DMX, dorsal motor nucleus of the vagus nerve; GLP-1R, glucagon-like peptide-1 receptor; lira^{VT750}, VivoTag750-S®-labeled liraglutide; LSc, lateral septal nucleus; ME, median eminence; MEPO, median preoptic nucleus; MM, medial mammillary nucleus; NTS, nucleus tractus solitarius; OV, vascular organ of the lamina terminalis; PVH, paraventricular nucleus of the hypothalamus; PVp, posterior part of PVH; SF, septofimbrial nucleus; SFO, subfornical organ; SO, supraoptic nucleus; TU, tuberal nucleus.

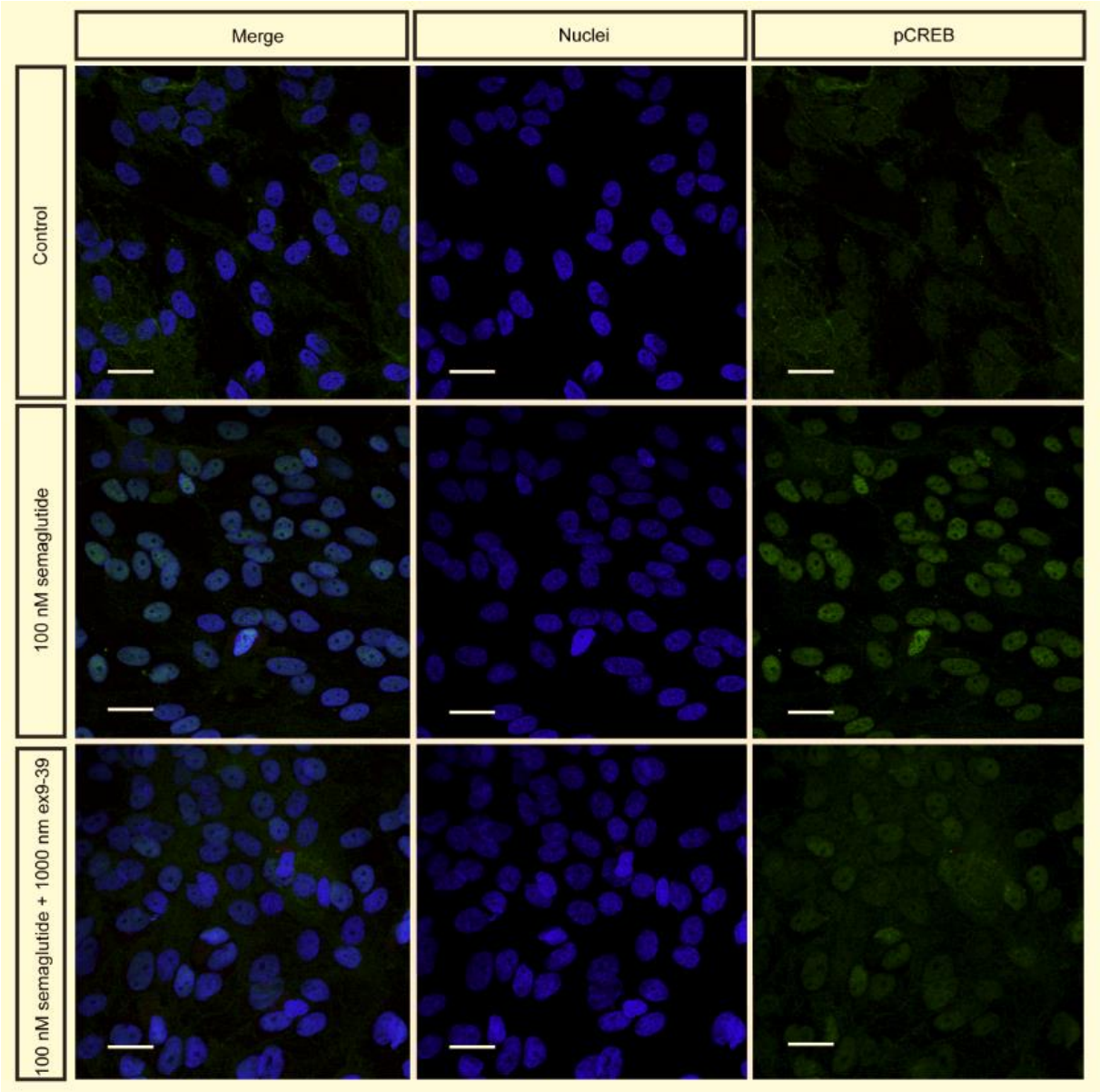

Supplementary Figure 3. In vitro activation of tanycytes with semaglutide. Rat tanycytes with 100 nM unlabeled semaglutide ± 1000 nM ex-9-39. Cells were stained for pCREB (green) and nuclei were counterstained with Hoechst (blue). Scale = 25 μm. ex-9-39, exendin 9-39; pCREB, phosphorylation of the cyclic AMP response element binding protein.

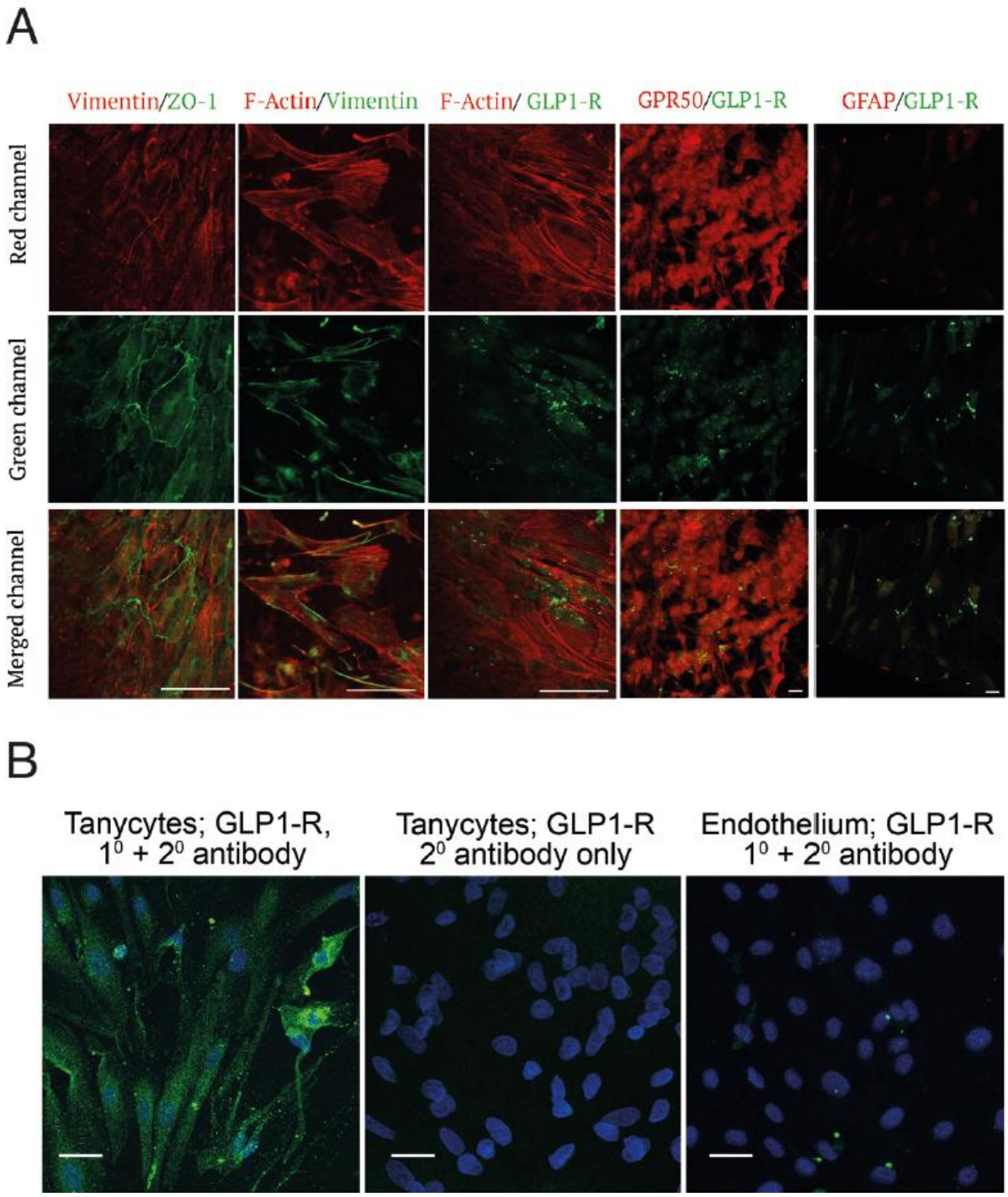

Supplementary Figure 4. Cell markers and GLP-1R expression in tanycytes. (A) Purity of the primary cultures of tanycytes is shown by the fact that most cells express the tanycytic marker GPR50 (column 4). Primary tanycytes are also seen to express vimentin (columns 1 and 2) and ZO-1 (column 1), but do not express the astrocytic marker GFAP (column 5). A subset of cultured tanycytes show immunoreactivity for GLP-1R (columns 3−5, green). Vimentin and F-actin show the cytoskeleton of the cells, while ZO-1 shows tight junction zones between the tanycytes. Importantly, GLP-1R was expressed in GPR50-positive cells (column 4), whereas these cells were free of GFAP

(column 5). Scale bars = 50 μm. **(B)** Tanycytes showed expression of GLP-1R (left column), while incubation with a secondary antibody alone gave no signal using the same settings (middle column). Rat brain endothelial cells showed little or no GLP1-R expression using the same settings (right column). Scale bars = 25 μm. F-actin, filamentous actin; GFAP, glial fibrillary acidic protein; GLP-1R, glucagon-like peptide-1 receptor; GPR50, green fluorescent protein 50; ZO-1, zonula occludens-1 (tight junction protein-1).

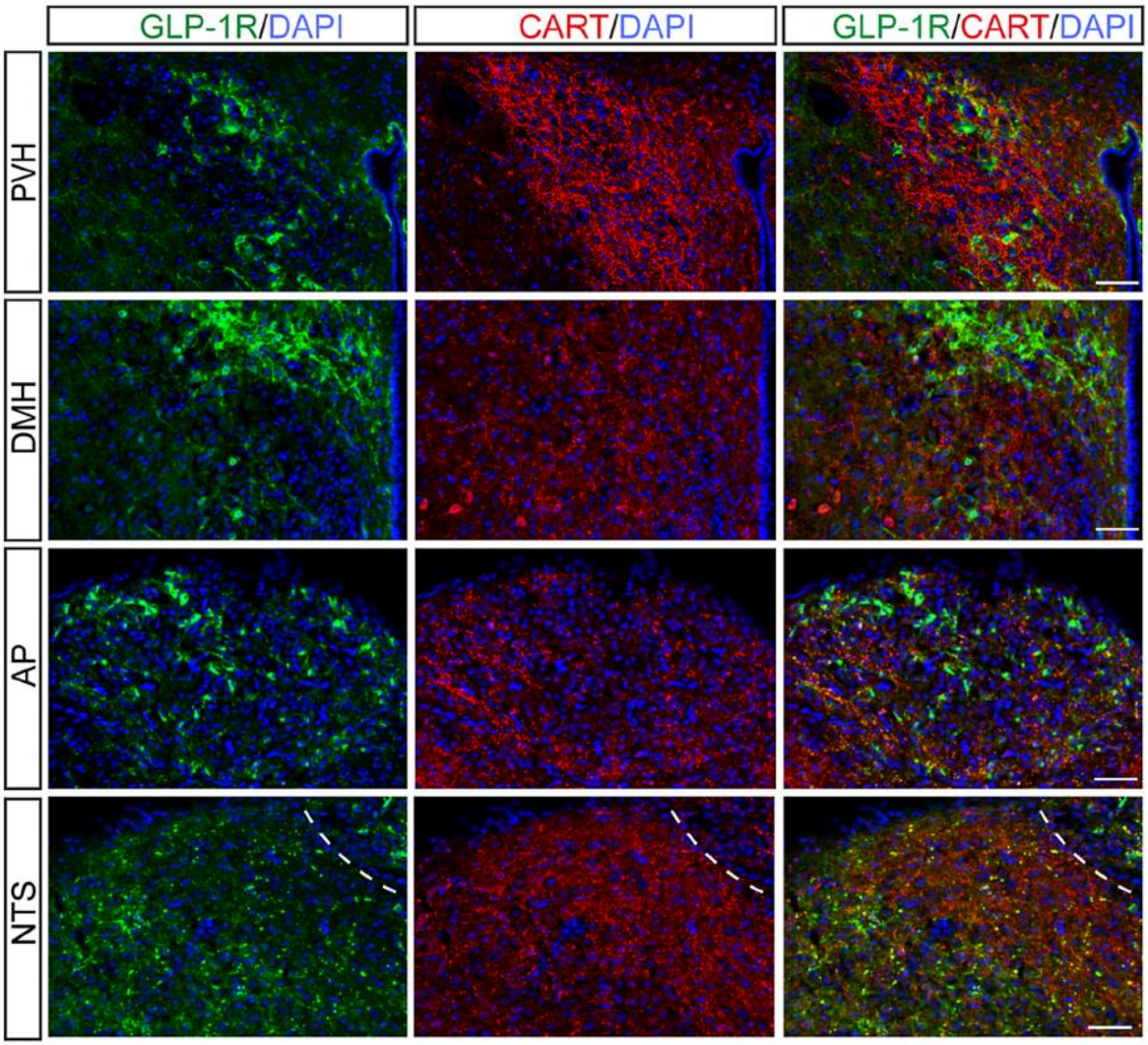

Supplementary Figure 5. GLP-1R and CART localization. Representative high-power immunofluorescence images taken from multiple regions immunofluorescently processed for both GLP-1R and CART. Panels illustrate GLP-1R (green), CART (red) together with DAPI nuclear staining (blue) and the merged image from the PVH, DMH, AP and NTS without the presences of co-expression in any of the regions. Dashed line designates the boundary between the NTS and the AP. Scale bars = 100 μm. AP, area postrema; CART, cocaine- and amphetamine-regulated transcript; DMH, dorsomedial hypothalamic nucleus; GLP-1R, glucagon-like peptide-1 receptor; NTS, nucleus tractus solitarius; PVH, paraventricular nucleus of the hypothalamus.

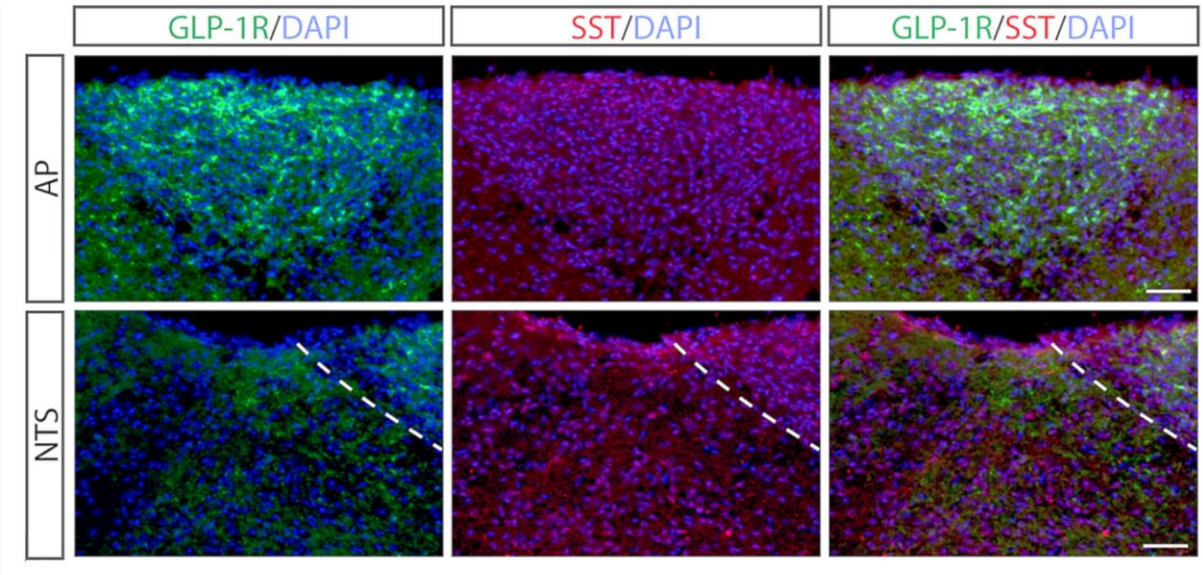

Supplementary Figure 6. GLP-1R and SST localization. Representative high-power immunofluorescence images taken from the hindbrain staining for GLP-1R and SST. Panels illustrate GLP-1R (green), SST (red) together with DAPI nuclear staining (blue) and the merged image from the AP and NTS without the presence of co-expression in any of the regions. Dashed line designates the boundary between the NTS and the AP. Scale bars = 100 μm. AP, area postrema; GLP-1R, glucagon-like peptide-1 receptor; NTS, nucleus tractus solitarius; SST, somatostatin.

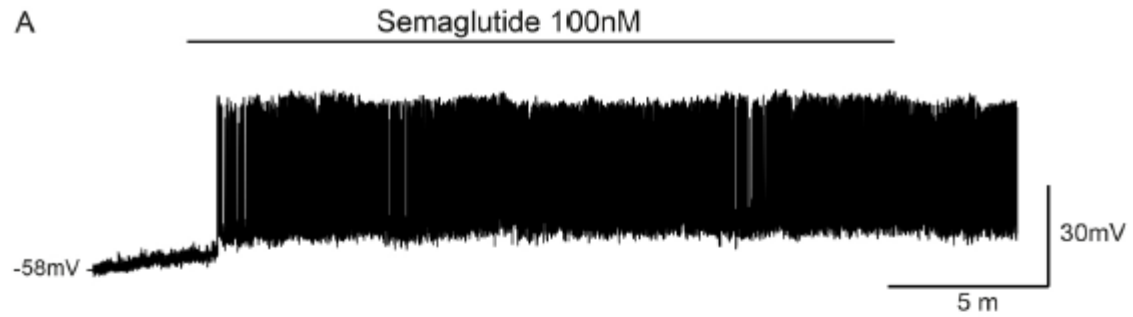
A
Semaglutide 100nM
-58mV
30mV
5 m

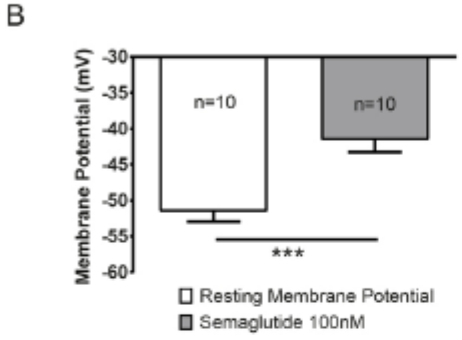
B
Membrane Potential (mV)
-30
-35
-40
-45
-50
-55
-60
n=10
n=10
***
Resting Membrane Potential
Semaglutide 100nM

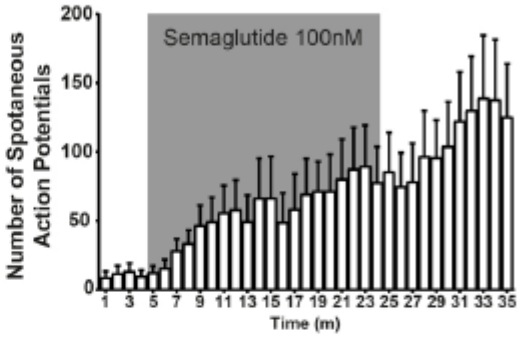
C
Number of Spotaneous Action Potentials
200
150
100
50
0
Semaglutide 100nM
1 3 5 7 9 11 13 15 17 19 21 23 25 27 29 31 33 35
Time (m)

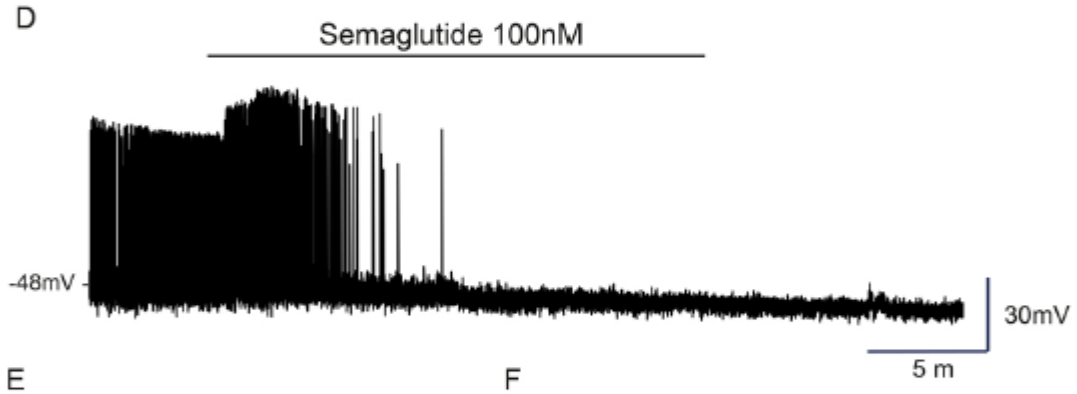
D
Semaglutide 100nM
-48mV
30mV
5 m

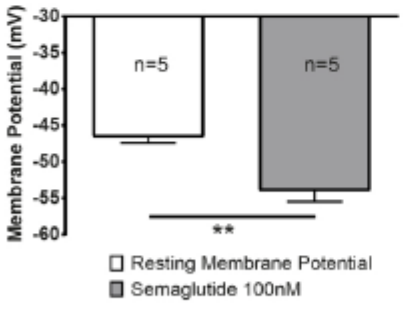
E
Membrane Potential (mV)
-30
-35
-40
-45
-50
-55
-60
n=5
n=5
**
Resting Membrane Potential
Semaglutide 100nM

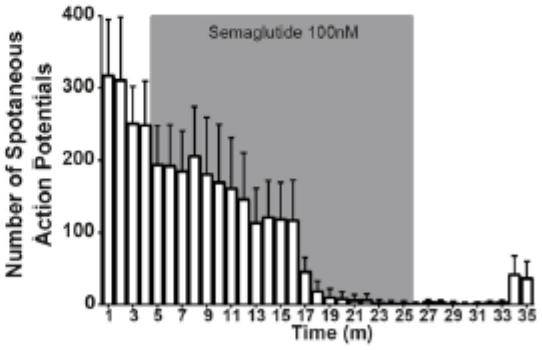
F
Number of Spotaneous Action Potentials
400
300
200
100
0
Semaglutide 100nM
1 3 5 7 9 11 13 15 17 19 21 23 25 27 29 31 33 35
Time (m)

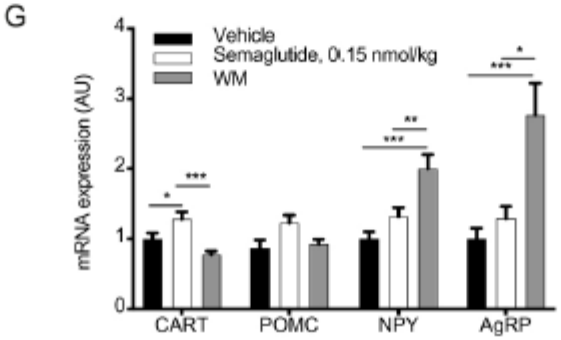
G
mRNA expression (AU)
4
3
2
1
0
Vehicle
Semaglutide, 0.15 nmol/kg
WM
*
***
**
***
*
***
CART
POMC
NPY
AgRP

Supplementary Figure 7. Effects of semaglutide in ARH neurons. (**A**) Representative trace from a POMC-enhanced green fluorescent protein (POMC-EGFP) neuron under current clamp recording in the presence of 100 nM semaglutide. Addition of semaglutide triggered membrane depolarization and increased the firing rate of POMC neurons. (**B**) Bar graph showing changes in the membrane potential following application of semaglutide. ***$P < 0.001$, paired t-test. (**C**) Histogram showing the effects of 100 nM semaglutide on the number of spontaneous action potentials in POMC neurons. (**D**) Representative trace from a neuropeptide-Y-green fluorescent protein (NPY-hrGFP) neuron under current clamp mode in the presence of 100 nM semaglutide. (**E**) Summary graph showing changes in membrane potential in NPY-hrGFP neurons after semaglutide application. **$P < 0.01$, paired t-test. (**F**) Histograms showing the effects of semaglutide in the firing rate of NPY-hrGFP neurons. Results are mean ± SEM. Resting membrane potential, paired *t* test. (**G**) qPCR data, expression of CART, POMC, NPY, and AgRP in the ARH of DIO mice administered once daily with vehicle or semaglutide, or weight-matched (WM) by food restriction to the semaglutide group (n=12/group). Data are mean ± SEM. AgRP, agouti-related peptide; ARH, arcuate nucleus; AU, arbitrary unit. DIO, diet-induced obese; CART, cocaine- and amphetamine-regulated transcript; NPY, neuropeptide-Y; POMC, pro-opiomelanocortin.

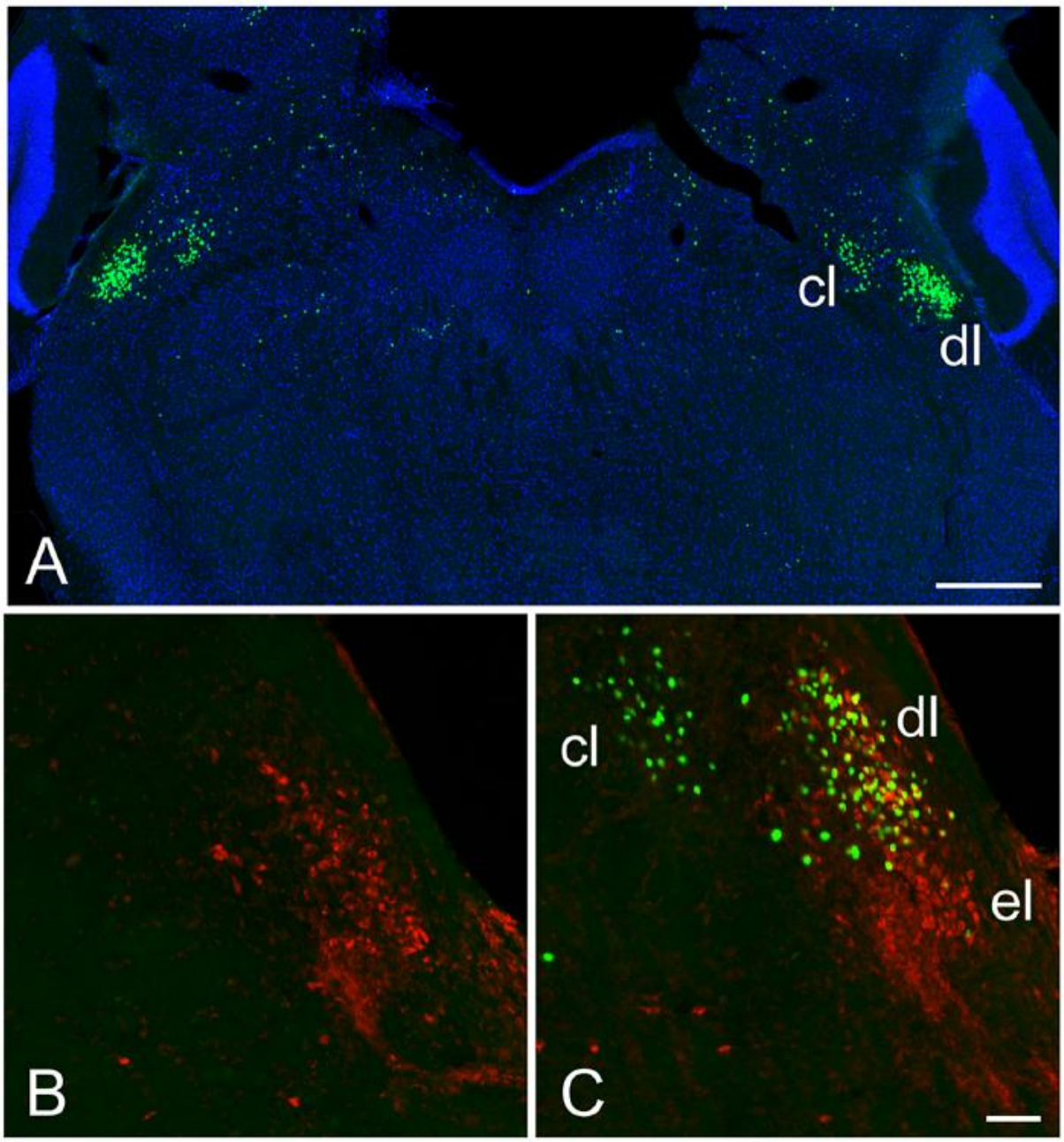

Supplementary Figure 8. Characterization of semaglutide-induced responses in the parabrachial nucleus. (**A**) Semaglutide-induced parabrachial nucleus (PB) c-Fos response showing c-Fos in the dorsal (dl) and central lateral (cl) subnuclei. Scale bar = 500 μm. (**B, C**) c-Fos and calcitonin gene-related peptide (CGRP) double immunofluorescence. CGRP-positive neurons were found in the dl and external lateral (el) PB. CGRP neurons in dl are c-Fos positive, whereas no c-Fos was found in the el. The c-Fos positive cl neurons do not express CGRP. Scale bar in C = 100 μm. Panels illustrate c-Fos (green), CGRP (red), with DAPI nuclear staining (blue).

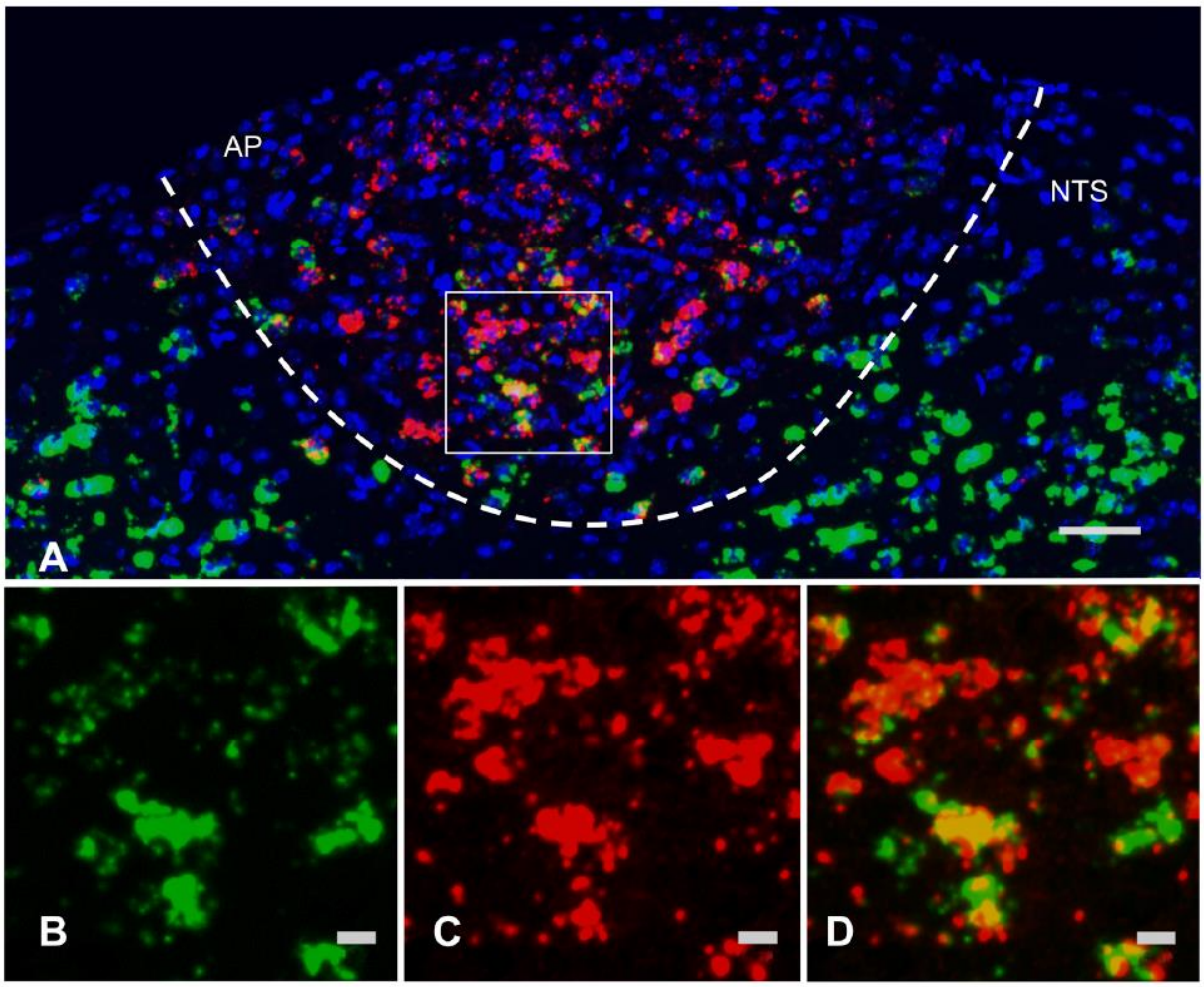

Supplementary Figure 9. Vesicular glutamate transporter SLC17A6 overlaps with GLP-1R positive cell bodies in the AP, but not the NTS. (**A**) Representative *in situ* hybridization image of vesicular glutamate transporter (SLC17A6, also known as vGLUT2; Green), GLP-1R (red), and DAPI staining in the hindbrain. Scale bar = 50 μm. (**B−D**) Single and composite images of the boxed region from A, showing SLC17A6 in a subset of GLP-1R-expressing cells in the AP. Scale bars = 10 μm. Dashed line indicates hypothetical boundaries between the AP and NTS. AP, area postrema; GLP-1R, glucagon-like peptide-1 receptor; NTS, nucleus tractus solitaries; vGLUT2, vesicular glutamate transporter.

A

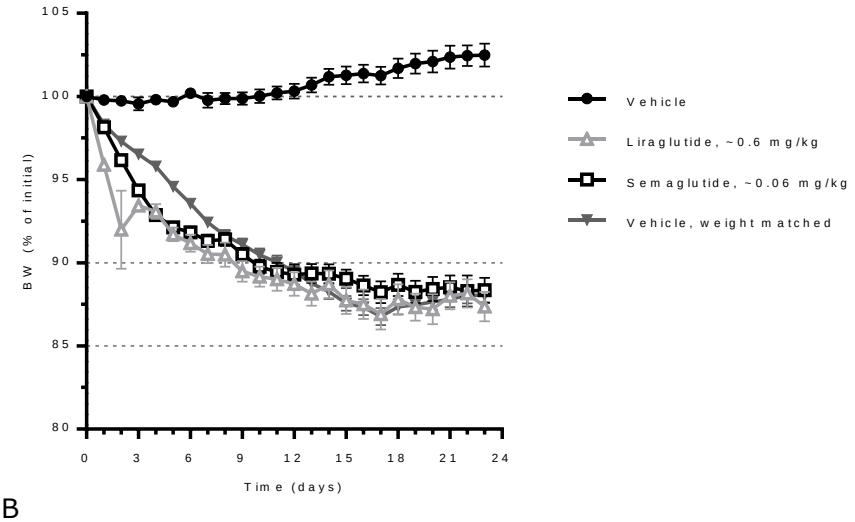
105
100
95
90
85
80
BW (% of initial)
0
3
6
9
12
15
18
21
24
Time (days)
Vehicle
Liraglutide, ~0.6 mg/kg
Semaglutide, ~0.06 mg/kg
Vehicle, weight matched

B

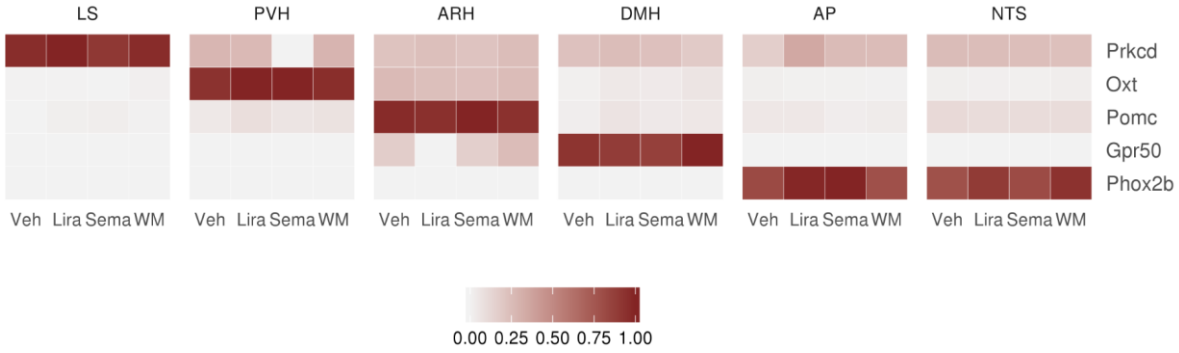
LS
PVH
ARH
DMH
AP
NTS
Prkcd
Oxt
Pomc
Gpr50
Phox2b
Veh Lira Sema WM
0.00 0.25 0.50 0.75 1.00

C

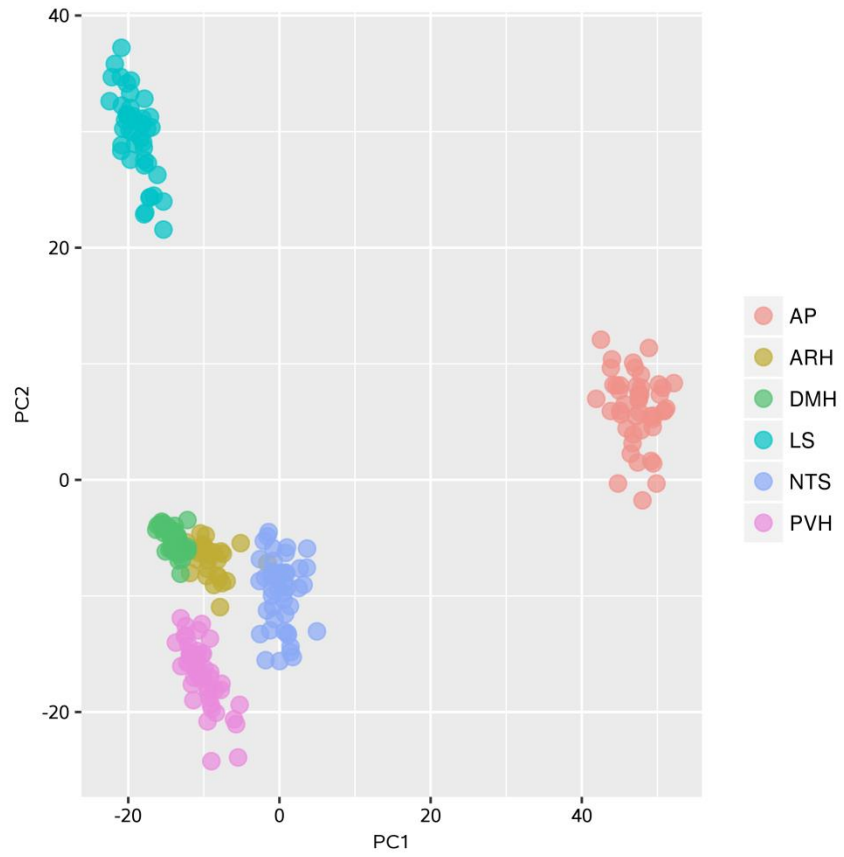
40
20
0
-20
PC2
-20
0
20
40
PC1
AP
ARH
DMH
LS
NTS
PVH

D

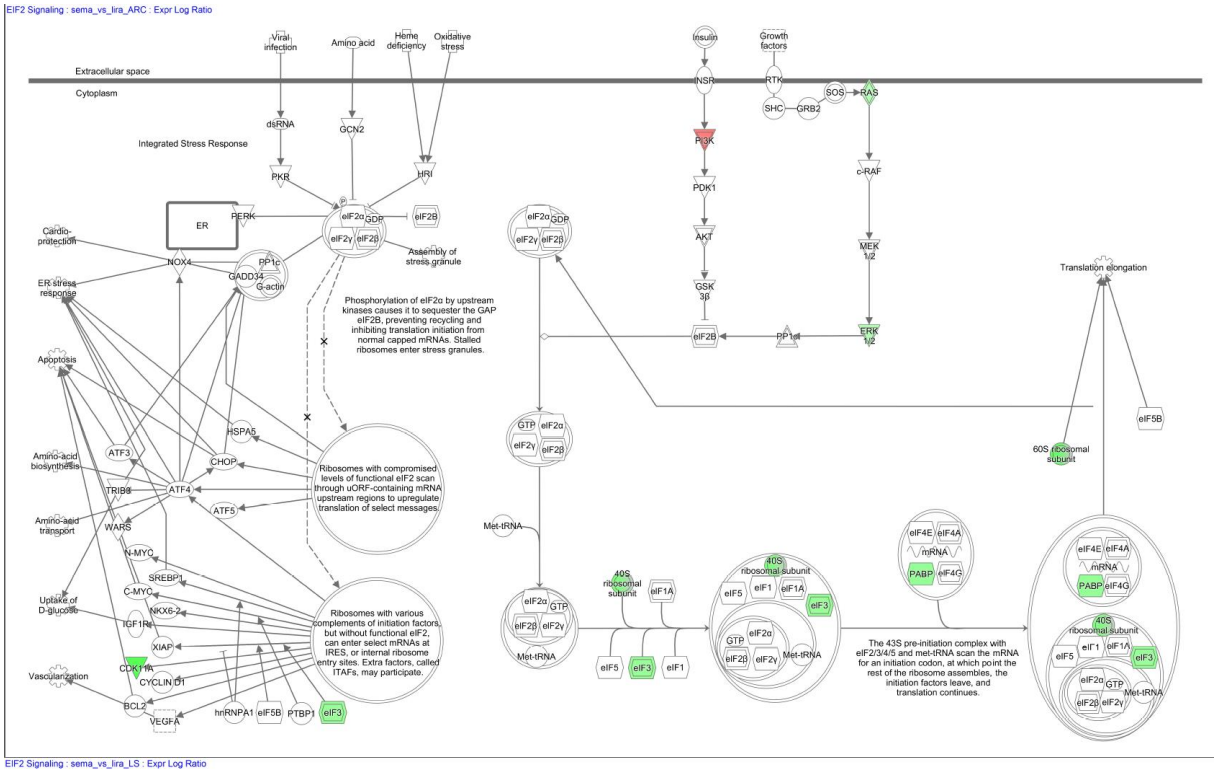
EIF2 Signaling : sema_vs_lira_ARC : Expr Log Ratio
Viral infection
Amino acid
Heme deficiency
Oxidative stress
Extracellular space
Cytoplasm
dsRNA
GCN2
Integrated Stress Response
PKR
HRI
ER
PERK
eIF2α GDP
eIF2γ eIF2β
eIF2B
Assembly of stress granule
Cardio-protection
NOX4
PP1c
GADD34
G-actin
ER stress response
Phosphorylation of eIF2α by upstream kinases causes it to sequester the GAP eIF2B, preventing recycling and inhibiting translation initiation from normal capped mRNAs. Stalled ribosomes enter stress granules.
Apoptosis
HSPA5
ATF3
CHOP
Amino-acid biosynthesis
TRIB3
ATF4
ATF5
Ribosomes with compromised levels of functional eIF2 scan through uORF-containing mRNA upstream regions to upregulate translation of select messages.
Amino-acid transport
WARS
N-MYC
SREBP1
C-MYC
Uptake of D-glucose
NKX6-2
IGF1Rα
XIAP
CDK1/A
CYCLIN D1
Vascularization
BCL2
VEGFA
Ribosomes with various complements of initiation factors, but without functional eIF2, can enter select mRNAs at IRES, or internal ribosome entry sites. Extra factors, called ITAFs, may participate.
hnRNPA1
eIF5B
PTBP1
eIF3
Insulin
Growth factors
INSR
RTK
SOS
RAS
SHC
GRB2
PI3K
c-RAF
PDK1
AKT
MEK 1/2
GSK 3β
eIF2B
PP1c
ERK 1/2
Translation elongation
eIF5B
60S ribosomal subunit
GTP eIF2α
eIF2γ eIF2β
Met-tRNA
40S ribosomal subunit
eIF1A
eIF5
eIF3
eIF1
eIF1
eIF4E eIF4A
mRNA
PABP eIF4G
The 43S pre-initiation complex with eIF2/3/4/5 and met-tRNA scan the mRNA for an initiation codon, at which point the rest of the ribosome assembles, the initiation factors leave, and translation continues.

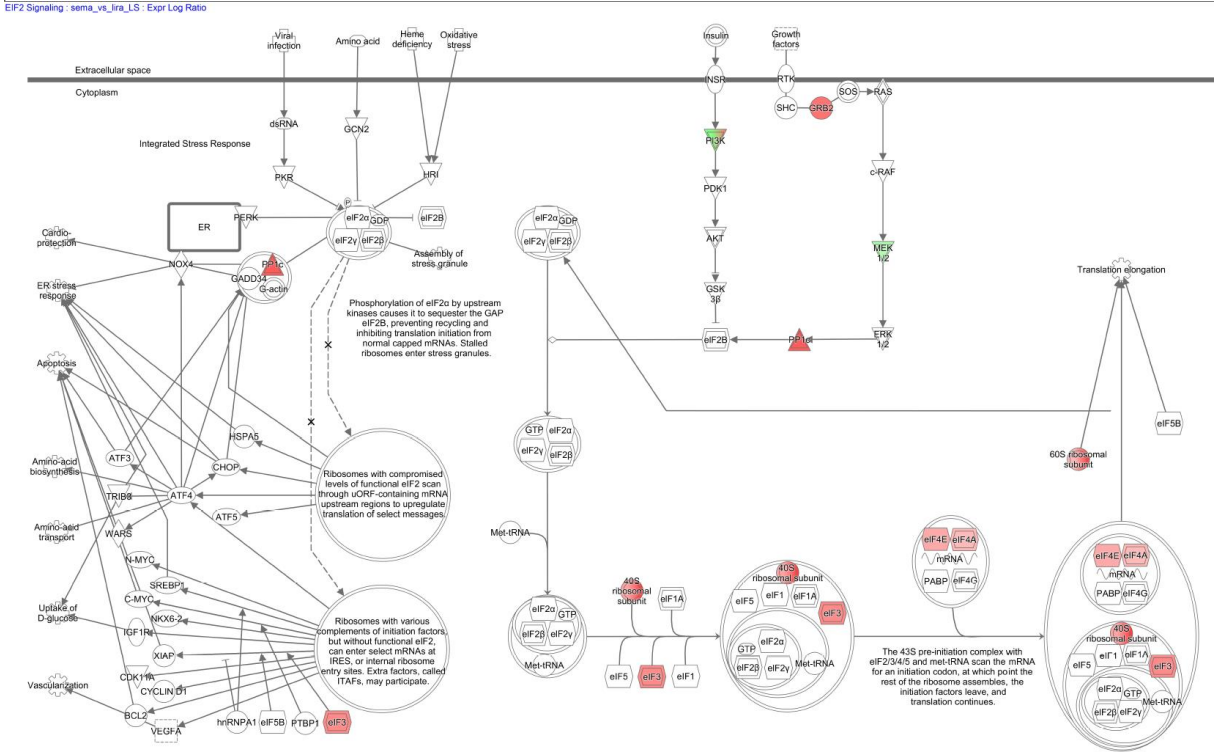
EIF2 Signaling : sema_vs_lira_LS : Expr Log Ratio
Viral infection
Amino acid
Heme deficiency
Oxidative stress
Extracellular space
Cytoplasm
dsRNA
GCN2
Integrated Stress Response
PKR
HRI
ER
PERK
eIF2α GDP
eIF2γ eIF2β
eIF2B
Assembly of stress granule
Cardio-protection
NOX4
PP1c
GADD34
G-actin
ER stress response
Phosphorylation of eIF2α by upstream kinases causes it to sequester the GAP eIF2B, preventing recycling and inhibiting translation initiation from normal capped mRNAs. Stalled ribosomes enter stress granules.
Apoptosis
HSPA5
ATF3
CHOP
Amino-acid biosynthesis
TRIB3
ATF4
ATF5
Ribosomes with compromised levels of functional eIF2 scan through uORF-containing mRNA upstream regions to upregulate translation of select messages.
Amino-acid transport
WARS
N-MYC
SREBP1
C-MYC
Uptake of D-glucose
NKX6-2
IGF1Rα
XIAP
CDK1/A
CYCLIN D1
Vascularization
BCL2
VEGFA
Ribosomes with various complements of initiation factors, but without functional eIF2, can enter select mRNAs at IRES, or internal ribosome entry sites. Extra factors, called ITAFs, may participate.
hnRNPA1
eIF5B
PTBP1
eIF3
Insulin
Growth factors
INSR
RTK
SOS
RAS
SHC
GRB2
PI3K
c-RAF
PDK1
AKT
MEK 1/2
GSK 3β
eIF2B
PP1c
ERK 1/2
Translation elongation
eIF5B
60S ribosomal subunit
GTP eIF2α
eIF2γ eIF2β
Met-tRNA
40S ribosomal subunit
eIF1A
eIF5
eIF3
eIF1
eIF1
eIF4E eIF4A
mRNA
PABP eIF4G
The 43S pre-initiation complex with eIF2/3/4/5 and met-tRNA scan the mRNA for an initiation codon, at which point the rest of the ribosome assembles, the initiation factors leave, and translation continues.

EIF2 Signaling : sema_vs_lira_PVN : Expr Log Ratio

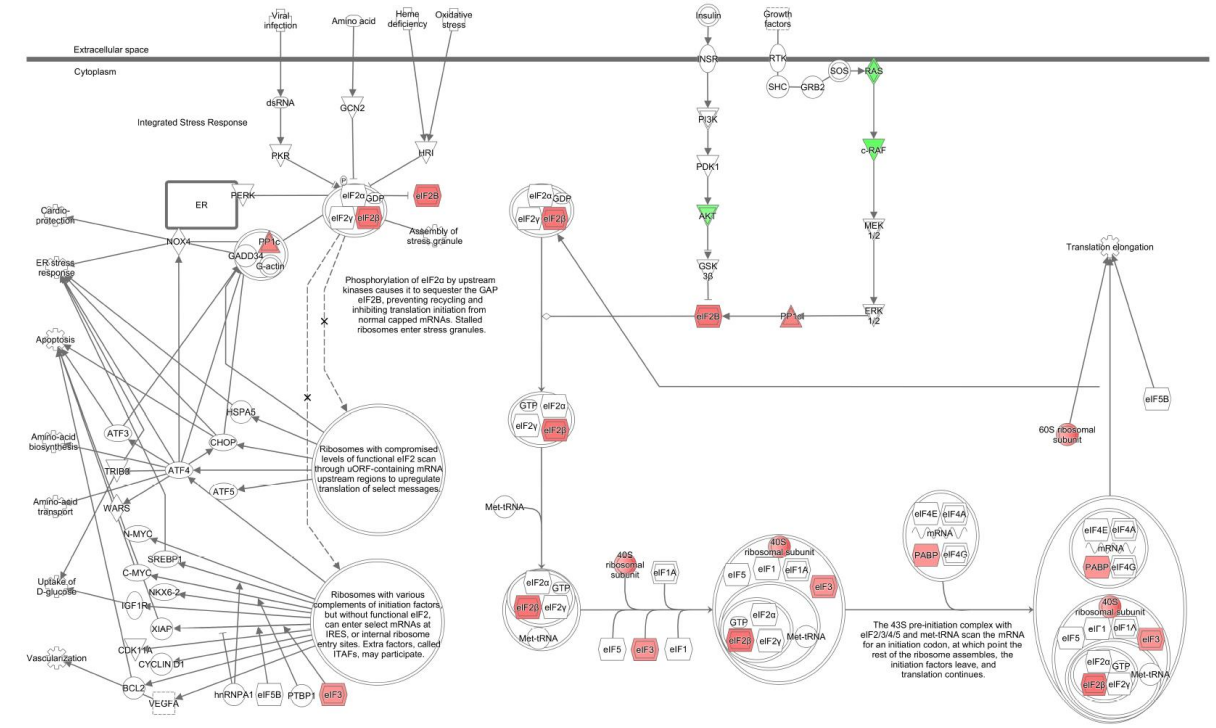

Oxidative Phosphorylation : sema_vs_lira_ARC : Expr Log Ratio

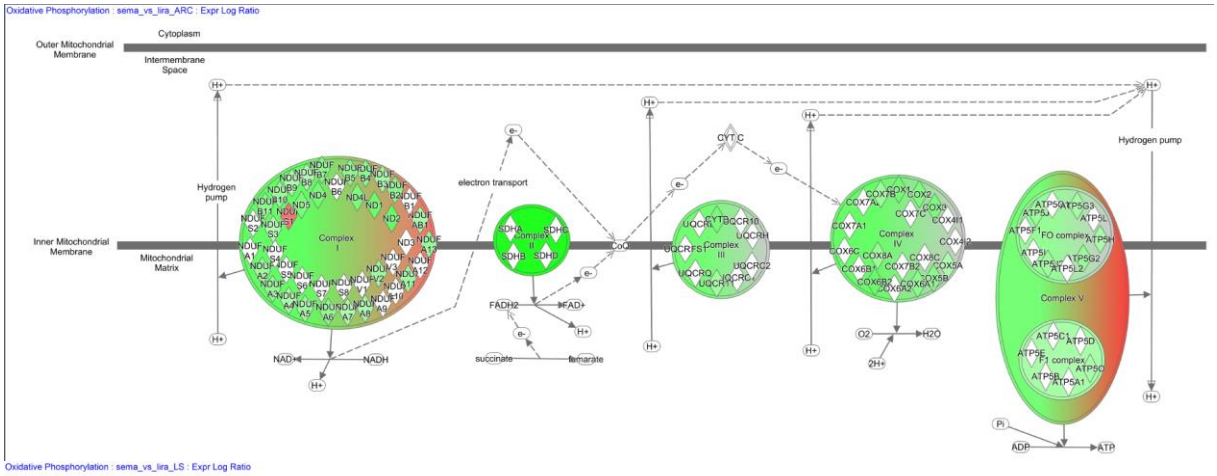

Oxidative Phosphorylation : sema_vs_lira_LS : Expr Log Ratio

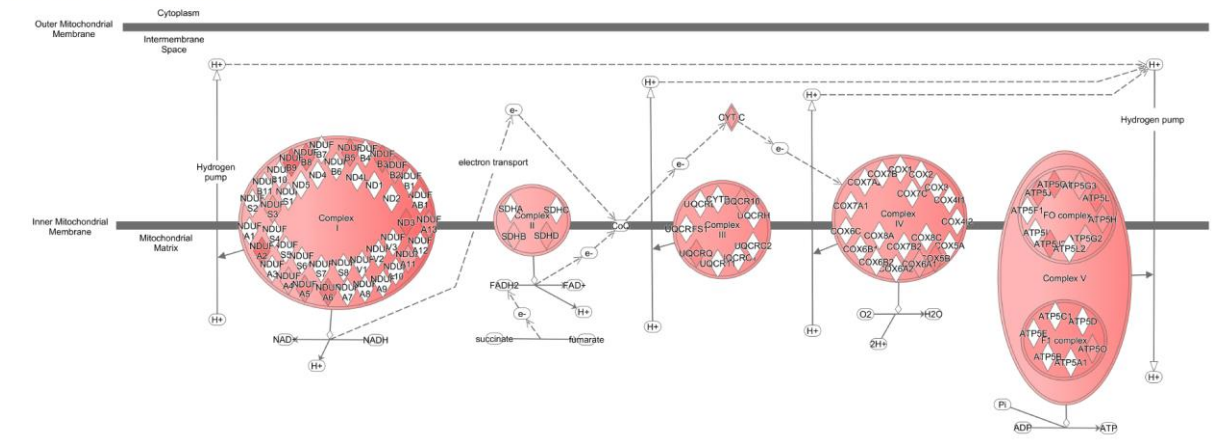

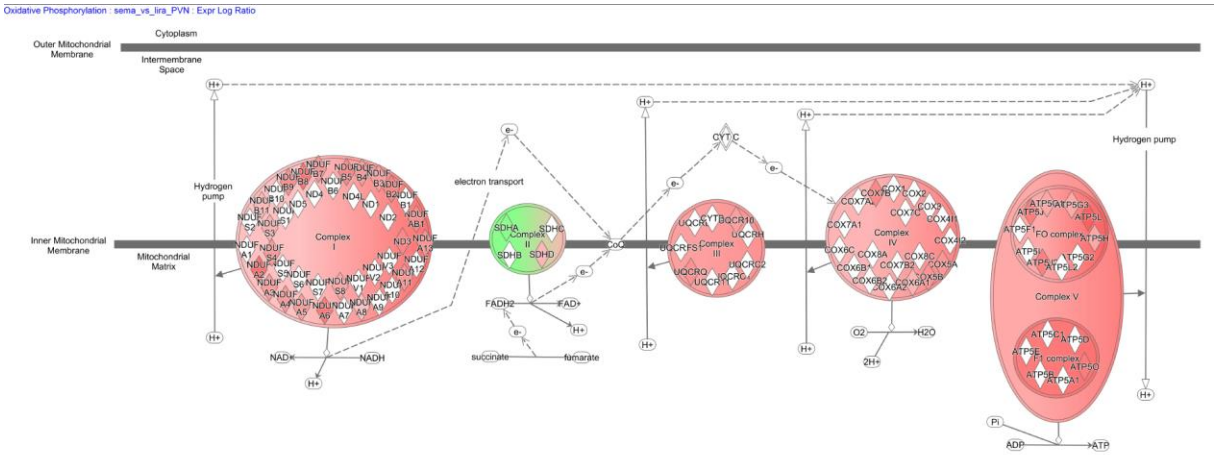

Supplementary Figure 10. Transcriptomic data. (**A**) Relative BW in percentage (%) per day in DIO rats treated once daily with vehicle, liraglutide, semaglutide, or weight-matched by food restriction to the semaglutide group (n=16/group). Data are mean ± SEM. (**B**) Heatmap showing expression of selected genes to assess laser capture microdissection (LCM) purity. For comparability, variance stabilized expression values have been scaled to between 0 and 1. (**C**) Principal component analysis of the top 1000 most variable genes across all included samples based on variance stabilized expression values. (**D**) Ingenuity Pathway Analysis (Qiagen Bioinformatics, Redwood city, USA) maps of the two canonical pathways: 'Oxidative Phosphorylation' and 'Eukaryotic Initiation Factor 2 signaling' ('EIF2 signaling') are shown for the ARH, lateral sulcus (LS) and PVH areas. Individual genes (with observed differences between liraglutide and semaglutide groups; uncorrected *P* value < 0.05) are color-coded based on their relative expression in liraglutide- and semaglutide-treated groups. Red indicates higher expression levels in semaglutide-treated animals, whereas green indicates higher expression in liraglutide-treated animals. For the oxidative phosphorylation pathway, individual complexes are likewise color-coded and a mix of green and red indicates that both genes with highest expression following liraglutide and semaglutide treatment were identified (not all individual genes shown for all complexes). AP, area postrema; ARH, arcuate nucleus; DIO, diet-induced obese; DMH, dorsomedial hypothalamic nucleus; GPR50, G-protein-coupled receptor 50; Lira, liarglutide; OXT, oxytocin; PHOX2B, paired-like homeobox 2b; POMC, pro-opiomelanocortin; PRKCD, protein kinase C delta; PVH, paraventricular nucleus of the hypothalamus; NTS, nucleus tractus solitarius; Sema, semaglutide; Veh, vehicle; WM, weight matched.

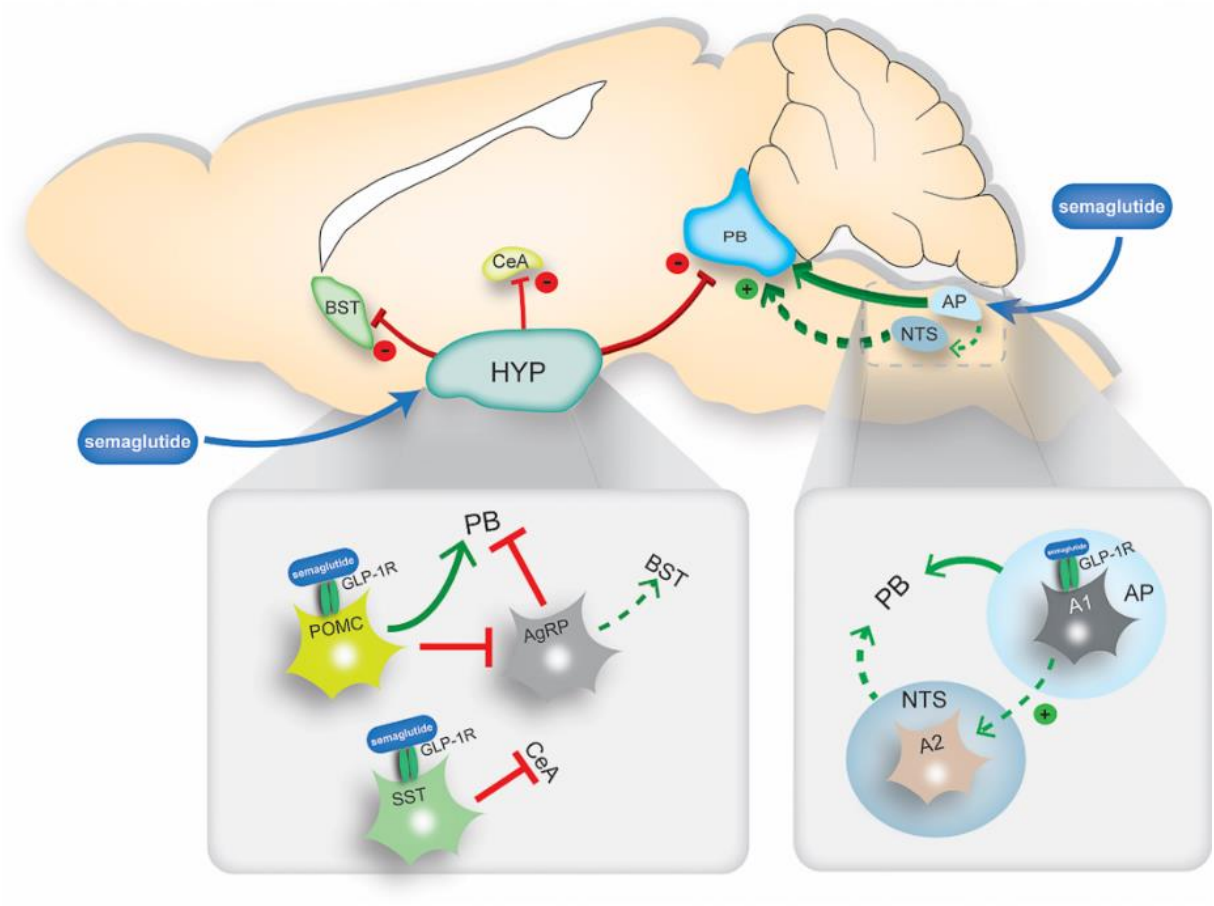

Supplementary Figure 11. Proposed primary and secondary brain activation pathways by semaglutide. Direct activation of GLP-1Rs by semaglutide occurs in the hindbrain (AP/NTS) and hypothalamus (ARH). It is hypothesized that semaglutide administration induces an AP/NTS-directed secondary neuronal response in the PB, either directly through GLP-1R stimulation of AP-to-PB projections or indirectly through the AP-to-NTS-to-PB pathway. The latter may occur through A1−A2 projections. The c-Fos signal can be further stimulated through activation of GLP-1R on POMC cells and through disinhibition of the AgRP inhibitory tone to the PB. c-Fos induction is also possible through projections of SST neurons to the CeA and AgRP neurons to the PB. A1/A2, noradrenegic cell group 1/2; AgRP, agouti-related peptide; AP, area prostrema; ARH, arcuate nucleus; BST, bed nuclei of the stria terminalis; CeA; central amygdala nucleus; GLP-1R, glucagon-like-1 receptor; HYP, hypothalamus; NTS, nucleus tractus solitarius; PB, parabrachial nucleus; POMC, pro-opiomelanocortin; SST, somatostatin.

Supplementary tables

Rank	Structure	Mouse line	Experiment id
1	NTS/DMX	Rasgrf2-T2A-dCre	310853453
2	GR/NTS	Gal-Cre_KI87	175816975
3	GR/NTS	C57BL/6J	159648854
4	GR/NTS/MDRNv	Slc6a5-Cre_KF109	128003477
5	NTS/DMX	Pnmt-Cre	155735108
6	NTS/DMX	Ppp1r17-Cre_NL146	268323342
7	NTS/DMX	Tac1-IRES2-Cre	180525136
8	PB	Calb2-IRES-Cre	183284388
9	PVH	Efr3a-Cre_NO108	299759881
10	PB	Chat-IRES-Cre-neo	264565965
11	CeA	C57BL/6J	112459547
12	PB	Npr3-IRES2-Cre	545427588
13	PB	Slc17a6-IRES-Cre	305404551
14	AHN	Nos1-CreERT2	304998039
15	CeA	Erbb4-T2A-CreERT2	120281646
16	PAG	Gad2-IRES-Cre	302053755
17	XII/MDRNv	C57BL/6J	127350480
18	PB	Chat-IRES-Cre-neo	183901489
19	CeA	Etv1-CreERT2	286774064
20	PB	C57BL/6J	268415561
21	XII	Chat-IRES-Cre-neo	165973664
22	CeA	Prkcd-GluCla-CFP-IRES-Cre	265945645
23	AHN	Slc18a2-Cre_OZ14	301673462
24	MEA	Cart-Tg1-Cre	168363874
25	PB/SUT	Adcyap1-2A-Cre	301016900
26	DMH	Sim1-Cre_KJ18	159222295
27	CeA/SI	C57BL/6J	146795148
28	CeA/MEA	Crh-IRES-Cre_ZJH	267152406
29	V	Chat-IRES-Cre-neo	166052101
30	XII	Chat-IRES-Cre-neo	177606140

Supplementary Table 1. Most overlapping connectivity maps from Allen Institute for Brain Science (AIBS). List of the 30 most overlapping connectivity maps from AIBS compared with the semaglutide-specific c-Fos increase following acute administration. The 'Structure' column indicates the primary injection site where the virus used to trace the connections was injected. The 'Mouse line' column indicates the mouse line used for the specific tracing experiment. The 'Experiment id' column shows the unique AIBS id number for each experiment. All connectivity maps were downloaded from the AIBS data portal. AHN, anterior hypothalamic nucleus; CeA, central amygdalar; GR, gracile nucleus; MDRNv, medullary reticular nucleus, ventral part; MEA, medial amygdalar nucleus; PAG, periaqueductal gray; SI, substantia innominate; SUT, supratrigeminal nucleus; V, trigeminal nucleus; XII, hypoglossal nucleus.

	LS		PVH		ARH		DMH		AP		NTS	
	P < 0.05	FDR < 0.05	*P* < 0.05	FDR < 0.05	*P* < 0.05	FDR < 0.05	*P* < 0.05	FDR < 0.05	*P* < 0.05	FDR < 0.05	*P* < 0.05	FDR < 0.05
Sema vs lira	910	0	774	1	1143	1	1101	0	230	0	324	0
Sema vs veh	261	1	290	0	405	0	591	0	319	1	257	0
Sema vs WM	248	0	324	0	484	2	608	7	309	1	335	0
Lira vs veh	539	0	609	4	792	2	884	0	327	3	272	0
Lira vs WM	712	5	568	1	1521	63	1022	4	291	1	227	1
Veh vs WM	250	0	180	0	536	0	569	0	257	0	289	0

Supplementary Table 2. Number of differentially expressed genes (DEGs) identified between the different treatment groups in each of the six brain areas analyzed using transcriptomic analysis. *P* < 0.05: DEGs with an uncorrected *P* value <0.05. FDR < 0.05: DEGs with an FDR < 0.05.

Supplementary Table 3. Median gene expression values and statistics for all genes and comparisons

- Please see Supplementary Excel file.

Supplementary videos

- Supplementary Video 1: semaglutide^{VT750} distribution in the mouse brain at steady state (after 5 days s.c. dosing).
- Supplementary Video 2: neuronal activation based on c-Fos staining following acute semaglutide administration.

References

1. Ertürk A, Becker K, Jährling N, Mauch CP, Hojer CD, Egen JG, et al. Three-dimensional imaging of solvent-cleared organs using 3DISCO. *Nat Protoc.* 2012;7(11):1983-95.
2. Renier N, Wu Z, Simon DJ, Yang J, Ariel P, and Tessier-Lavigne M. iDISCO: a simple, rapid method to immunolabel large tissue samples for volume imaging. *Cell.* 2014;159(4):896-910.
3. Hertz L, Juurlink BHJ, Hertz E, and Fosmark H. In: Shahar A, Vellis JVAD, and Haber B eds. *A Dissection and Tissue Culture Manual of the Nervous System*. New York: Alan R. Liss, Inc; 1989:105-8.
4. Helms HC, and Brodin B. Generation of primary cultures of bovine brain endothelial cells and setup of cocultures with rat astrocytes. *Methods Mol Biol.* 2014;1135:365-82.
5. Prevot V, Cornea A, Mungenast A, Smiley G, and Ojeda SR. Activation of erbB-1 signaling in tanycytes of the median eminence stimulates transforming growth factor beta1 release via prostaglandin E2 production and induces cell plasticity. *J Neurosci.* 2003;23(33):10622-32.
6. Ballet S, Betti C, Novoa A, Tomboly C, Nielsen CU, Helms HC, et al. In vitro membrane permeation studies and in vivo antinociception of glycosylated Dmt-DALDA analogues. *ACS Med Chem Lett.* 2014;5(4):352-7.
7. Helms HC, Madelung R, Waagepetersen HS, Nielsen CU, and Brodin B. In vitro evidence for the brain glutamate efflux hypothesis: brain endothelial cells cocultured with astrocytes display a polarized brain-to-blood transport of glutamate. *Glia.* 2012;60(6):882-93.
8. Hersom M, Helms HC, Pretzer N, Goldeman C, Jensen AI, Severin G, et al. Transferrin receptor expression and role in transendothelial transport of transferrin in cultured brain endothelial monolayers. *Mol Cell Neurosci.* 2016;76:59-67.

9. Paxinos G, and Franklin KBJ. *Paxinos and Franklin's The Mouse Brain in Stereotaxic Coordinates.* Oxford: Academic Press; 2012.
10. Paxinos G, and Watson C. *The Rat Brain in Stereotaxic Coordinates.* London: Academic Press; 2013.
11. Livak KJ, and Schmittgen TD. Analysis of relative gene expression data using real-time quantitative PCR and the 2(-Delta Delta C(T)) Method. *Methods.* 2001;25(4):402-8.
12. Schmieder R, and Edwards R. Quality control and preprocessing of metagenomic datasets. *Bioinformatics.* 2011;27(6):863-4.
13. Dobin A, Davis CA, Schlesinger F, Drenkow J, Zaleski C, Jha S, et al. STAR: ultrafast universal RNA-seq aligner. *Bioinformatics.* 2013;29(1):15-21.
14. Love MI, Huber W, and Anders S. Moderated estimation of fold change and dispersion for RNA-seq data with DESeq2. *Genome Biol.* 2014;15(12):550.
15. Salinas CBG, Lu TT, Gabery S, Marstal K, Alanentalo T, Mercer AJ, et al. Integrated brain atlas for unbiased mapping of nervous system effects following liraglutide treatment. *Sci Rep.* 2018;8(1):10310.